Unione Europea

REGIONE CAMPANIA

P.O.R. Campania FSE 2007-2013

La tua Campania cresce in Europa

UNIVERSITÀ DEGLI STUDI DI NAPOLI FEDERICO II

Department of Mathematics and Applications "Renato Caccioppoli"

School of Doctoral Research in Computational and Information Sciences

SYSTEM IDENTIFICATION OF HORIZONTAL AXIS WIND TURBINES

CANDIDATE

Luigi Caracciolo di Torchiarolo

ACADEMIC TUTOR

Prof. Gioconda Moscariello

SCIENTIFIC TUTOR

Prof. Domenico Coiro

BUSINESS TUTOR

Dr. Ferdinando Scherillo

ABSTRACT

This thesis work is concerned with the identification of the aerodynamic characteristics, namely the lift and the drag coefficients of the airfoils placed along the blades, of horizontal axis wind turbines.

A wind turbine is represented by a quite complex dynamic system, composed in turn by several subsystems, for example aerodynamic, mechanical and electrical. It operates in stochastic and turbulent wind conditions and it gives rise to several complex phenomena, for example aeroelastic and three dimensional effects, dynamic stall, interactions between blades and tower as well as with other turbines within wind farms, etc.

There are several models, which represent the behaviour of a wind turbine. However, such models are characterized by the values that some curves assume. These curves must be suitably regulated [11] to obtain a better comparison between experimental data and the data produced by the mathematical model.

The purpose of this regulation is represented by the possibility to include some corrections related to the physical phenomena that have not been described by the mathematical model. This regulation also allows for accounting for manufacturing errors during the production of the blades.

The target of this work is precisely to find a reliable method which allows to calculate the aerodynamic curves of such wind turbines. However, the problem of system identification applied to wind turbines is hard to face. In fact, the causes underlying such difficulties, for example the low level of identifiability and

collinearity among parameters, prevents the calculation of such parameters. The problem is described in details in chapter 4 together with some methods used to solve the identification problem of wind turbines.

To this end a software package, written in MATLAB® [18] language, was created. This software implements the methods of system identification and calculates the required curves as described in chapter 4. To verify this software several tests were performed. Firstly, some tests using virtual experimental measurements have been performed to confirm the reliability of the generated curves. Then a test in which the identification is lost can be observed. The reasons that lead this software to gain a faulty solution or to not converge at all, instead of obtaining the real solution, are described in chapter 4. Finally other tests were conducted using the performance obtained from some experimental measurements in order to identify the aerodynamic characteristics of some real wind turbines.

SOMMARIO

Questo lavoro di tesi riguarda l'identificazione parametrica (system identification) delle proprietà aerodinamiche, ovvero dei coefficienti di portanza e di resistenza dei profili posizionati lungo le pale, di turbine eoliche ad asse orizzontale. Una turbina eolica è rappresentata da un sistema dinamico estremamente complesso, composto a sua volta da diversi sottosistemi, ad esempio aerodinamico, meccanico, elettrico. Essa opera in condizioni di vento stocastiche e turbolenti e da origine a fenomeni piuttosto complicati, ad esempio fenomeni aeroelastici, effetti tridimensionali, stallo dinamico, ad interazioni tra le pale e la torre, interazioni con altre turbine all'interno di parchi eolici, etc.

Esistono numerosi modelli in grado di rappresentare il comportamento di una turbina eolica. Tuttavia tali modelli sono caratterizzati dai valori assunti da alcune curve. Tali curve devono essere opportunamente calibrate al fine di ottenere un migliore riscontro tra i dati sperimentali e quelli ricavati dal modello matematico.

Lo scopo di queste regolazioni è rappresentato dalla possibilità di includere alcune correzioni relative a fenomeni fisici che non sono stati descritti dal modello matematico di riferimento. Tali regolazioni consentono inoltre di tenere conto degli errori durante la produzione delle turbine eoliche.

L'obiettivo di questo lavoro è proprio quello di trovare un metodo affidabile che consenta di calcolare le curve aerodinamiche di tali turbine eoliche. Tuttavia, il problema dell'identificazione

parametrica, applicato alle turbine eoliche, è difficile da affrontare. Infatti, le cause che sono alla base di queste difficoltà, ad esempio il basso livello di identificabilità, e la collinearità tra i parametri, impediscono il calcolo di tali curve. Il problema è descritto nei dettagli nel capitolo 4 insieme ad alcuni metodi usati per risolvere il problema dell'identificazione.

A tal fine è stato creato un software, scritto in linguaggio MATLAB® che implementa i metodi dell'identificazione parametrica e calcola le curve richieste come descritto nel capitolo 4. Per verificare il programma sono stati condotti numerosi test. All'inizio saranno effettuati alcuni test usando misure virtuali per confermare l'affidabilità delle curve trovate. Successivamente sarà presentato un test nel quale l'identificazione non è avvenuta con successo. Le ragioni che portano tale software ad ottenere una soluzione sbagliata o a non convergere affatto, invece di raggiungere la soluzione reale, sono spiegate nel capitolo 4. Infine saranno compiuti altri test utilizzando le prestazione ottenute da misure sperimentali al fine di identificare le curve aerodinamiche di alcune turbine eoliche reali.

CONTENTS

1 INTRODUCTION 1

2 AERODYNAMIC MODELS OF WIND TURBINES 7

2.1 Actuator disc model 8

2.2 Momentum Theory 10

2.3 General momentum theory 14

2.4 Blade element theory 16

2.5 The blade element momentum theory 19

2.6 Limits of the blade element momentum 20

2.7 Tip and root losses 21

2.8 Viterna Corrigan Model 23

3 SYSTEM IDENTIFICATION THEORY 27

3.1 Introduction 27

3.2 Mathematical modeling 28

3.3 Parameter estimation 29

3.3.1 Estimator for the Least-Squares model 31

3.3.2 Estimator for the Fisher model 32

3.3.3 Estimator for the Bayesian model 34

3.4 Cost function optimization algorithm 35

3.4.1 Relaxation strategy 35

3.4.2 Gauss-Newton method 36

3.4.3 Method of quasi-linearization 38

3.5 Properties of the estimates 39

3.6 Detection of data collinearity 41

3.6.1 Correlation matrix 41

3.6.2 Singular value decomposition 42

4 IDENTIFICATION OF WIND TURBINES 47

4.1 Geometry parametrization 56
4.1.1 Bezier Curves 57
4.2 Virtual identification 62
4.2.1 Identification of the lift coefficient 62
4.2.2 Identification of the lift and the drag coefficients 64
4.2.3 Identification of the aerodynamic characteristics of two airfoils 65
4.2.4 A simple case in which the identification of the aerodynamic characteristics is lost 68
4.3 Identification from experimental data 70
4.3.1 Identification of the lift coefficient 71
4.3.2 Identification of the lift and the drag coefficients 72
4.3.3 Identification of the aerodynamic characteristics of two airfoils 72
4.4 Identification of the wind turbine EOL-H-60 77
4.4.1 Identification of the lift coefficient 78
4.4.2 Identification of the lift and the drag coefficients 78
4.4.3 Conclusions 79

BIBLIOGRAPHY 83

LIST OF FIGURES

Figure 1 Wind turbine stream tube 9

Figure 2 Actuator disc model 11

Figure 3 Blade element operating condition 17

Figure 4 Prandtl tip-root losses factor 23

Figure 5 Typical characteristic curves 53

Figure 6 Typical aerodynamic curves 54

Figure 7 Example of Bezier curves 59

Figure 8 Convex hull of a Bezier curve 59

Figure 9 Identification of the lift coefficient of a wind turbine. Solid lines: identified curves; dashed lines: *virtual* experimental curves; dotted lines: initial curves. 63

Figure 10 particular of the identified lift curve 64

Figure 11 Identification of the lift coefficient and the drag coefficient of a wind turbine. Solid lines: identified curves; dashed lines: *virtual* experimental curves; dotted lines: initial curves. 65

Figure 12 Identification of the lift coefficient and the drag coefficient of a wind turbine. Solid lines: identified curves; dashed lines: *virtual* experimental curves; dotted lines: initial curves. 67

Figure 13 Failure of an identification of the lift coefficient of a wind turbine. Solid lines: identified curves; dashed lines: *virtual* experimental curves; dotted lines: initial curves. 69

Figure 14 Identification of the lift coefficient of the Bora wind turbine. Solid lines: identified curves; points: experimental data; dotted lines: initial curves. 71

Figure 15 Identification of the lift coefficient and the drag coefficient of the Bora wind turbine. Solid lines: identified curves; points: experimental data; dotted lines: initial curves. 73

Figure 16 Identification of the lift coefficient and the drag coefficient of the Bora wind turbine. Solid lines: identified curves; points: experimental data; dotted lines: initial curves. 74

Figure 17 Identification of the lift coefficient and the drag coefficient of the Bora wind turbine. Solid lines: identified curves; points: experimental data; dotted lines: initial curves. 76

Figure 18 Discrepancies between experimental and predicted data of the wind turbine Eol-H-60. Triangles: experimental data; dotted line: predicted curve. 77

Figure 19 Identification of the lift coefficient of the EOL-H-60 wind turbine. Solid lines: identified curves; triangles: experimental data; dotted lines: initial curves. 79

Figure 20 Identification of the lift and the drag coefficients of the EOL-H-60 wind turbine. Solid lines: identified curves; triangles: experimental data; dotted lines: initial curves. 80

Figure 21 Particular of the identified lift curve. Solid line: identified curve; dotted line: numerical curve. 81

Figure 22 Discrepancies between experimental and predicted data of the wind turbine Eol-H60 after the adjustments of the blades. Triangles: experimental data before corrections; diamonds: experimental data after corrections; dotted line: predicted numerical curve. 82

1

INTRODUCTION

In recent years the worldwide concern for the rise of CO_2 concentrations on earth atmosphere together with the oil price hike, have led to a fast-growing development of renewable energies, in particular of wind turbines, mainly thanks to the government policy, which has invested a lot of funds to decrease the dependence on fossil fuel and to reduce the concentrations of greenhouse gases.

The growth of several wind farms, and consequently the increase of installed power, is favoured by the possibility to extract a greater amount of energy from the wind to obtain greater yield. So, it is fundamental to acquire a mathematical model which will accurately represent the physics of the system under test. However it is also fundamental to fit, in the best possible way, the parameters which describe such a system.

Sometimes it may occur that the predicted performance of a design for a wind turbine differs significantly from those obtained through experimental measurements. These discrepancies can depend on several factors.

Firstly they can depend on some assumptions within the chosen aerodynamic models that can be not fully satisfied. The most important aerodynamic model used by the designers of wind turbines is the blade element momentum theory. This model is used mostly for its simplicity, for its low computational efforts and because it is able to get most out of the physics related to the wind turbines.

The theory related to this model, with its assumptions and its results, will be presented in details in chapter 2. The limitations of the model, determined by the assumptions that makes the model only an approximation of the real process and that cause the discrepancies between predicted and experimental data, are also discussed. Finally, some classical improvements are described in order to increase the fidelity of the model in performance prediction.

As pointed out in [11], several studies demonstrated that the main source of errors in evaluating the loads of the blades, and consequently in the performance prediction, is due to the wrong aerodynamic characteristics of the airfoils used along the blades span. But it is also emphasized that, to date, a reliable method which improves the fidelity of the characteristics of the airfoils does not exist.

Tangler in [17] has also verified that there are more discrepancies due to the use of different airfoils characteristics than those due to the employment of different simulation codes for performance predictions. This means that the choice among the prediction codes is less important than a suitable choice of the airfoils characteristics. For this reason the blade element momentum model will be used in this thesis work instead of other more complex codes, based for example on the lifting line theory, for performance prediction.

In addition, manufacturing errors represent another factor that may cause the discrepancies between design and experimental performance. In this case, despite of the fact that the modern technology has allowed for excellent industrial equipment, the presence of manufacturing errors in the created blades is unavoidable. These errors cause the alteration of the aerody-

namic airfoils characteristics and therefore the performance of wind turbines. A great part of the discrepancies between the predicted and the experimental data of the 60kW wind turbine called EOL-H-60 is precisely due to manufacturing errors. The identification of the aerodynamic characteristics carried out using the software developed in this thesis work helped to find the sources that caused the discrepancies and thus it helped to fix these errors. This problem is described in details in section 4.4. Other alterations are due, for example, to the roughness of the airfoils, which change its characteristics and therefore the performance of wind turbines.

The methods of system identification applied to wind turbines, are used to solve both problems at the same time. Indeed the aerodynamic data tables, calibrated in an appropriate way, allows to include both three-dimensional effects and manufacturing errors as well.

The theory related to the problem of system identification is presented in chapter 3. The methods of the parameter estimation are also described since the problem of system identification can be reduced to parameter estimation. In addition, the main estimators will be presented and more particularly the estimator for the Fisher model, which uses the likelihood function, will be described in details. Indeed the maximum likelihood estimator will be used in this thesis work in order to identify the aerodynamic characteristics of wind turbines under study. Then, the principal algorithms used to optimize the cost function given by the estimator model, will be described and implemented in the software created for this thesis work. The properties of the estimates will be presented and finally the problem of data collinearity will be described. The main tech-

niques used to avoid data collinearity, or at least to decrease its effects, are also discussed since the identification of wind turbines is strongly affected by this problem. A fundamental technique described in this thesis work and implemented in the software is the singular value decomposition. This method is able to detect the parameters that cause the failure of the optimization code so that the user can exclude them from the optimization giving the possibility to obtain better estimates. It precisely creates a new vector of parameters. The choice of the parameters to be optimized can either be made beforehand by the developer, who is helped by the Cramer-Rao bounds, or be leaved to the user, who can decide depending on the variance of the parameters he can accept, as explained in the proper section.

These techniques will be applied in chapter 4 in which the attention is focused on the identification of the aerodynamic properties of wind turbines and in particular on the choice of suitable representations of the aerodynamic curves which give the possibility to obtain better estimates for the curves themselves. Since, as pointed out, the problem of system identification applied to a wind turbine is very difficult to solve, different representations are proposed. The cause of this difficulty, as described in chapter 4, is due to the low level of identifiability that unavoidably occurs when the number of parameters is increased. On the other hand a great number of parameters is needed to model in a suitable way the aerodynamic properties of the given wind turbine, represented by the aerodynamic curves (the lift and the drag coefficients) at the several stations. Therefore a balance between the degrees of approximation of the aerodynamic curves and the need of reducing the correla-

tions among parameters has to be found by choosing the proper number of parameters which in turn depends on the availability of experimental measurements and on the quality of them. Tests conducted in chapter 4 confirm that if the number of identified curves increases, the quality of the resulting estimates is reduced.

2

AERODYNAMIC MODELS OF WIND TURBINES

In this chapter the basic aerodynamic theory is presented in order to analyse the behaviour of a wind turbine, which is a device exploited to convert the kinetic energy present in the atmosphere into mechanical energy and, in our particular case, into electrical energy.

The creation of a comprehensive model for a wind turbine is a very difficult task. In fact a viscous, unsteady and compressible flow field needs to be considered as well as a statistical study to account for the randomness of wind.

For a complete discussion on how a wind turbine works, several excellent books (for example [3, 19]) can be found in the literature. From these books a better knowledge on wind turbines can be acquired since some details, not strictly necessary in this treatise, are neglected.

The models that will be presented in this chapter have been implemented in some prediction codes which allow to obtain the performance of a given wind turbine. The prediction codes used in this thesis work are ELICA, developed in FORTRAN language on the basis of the PROPPC code [16] at the ADAG group of DIAS of the UNIVERSITY OF NAPLES FEDERICO II, and the faster WTPERF, developed by the NATIONAL RENEWABLE ENERGY LABORATORY (NREL) [15].

More comprehensive models could be considered in order to improve the identification of the aerodynamic characteristics. For example, models taking into account the flexibility of the

blades and that can see the variation of the blade elements angles of attack and therefore can better calculate the performance of the given wind turbine. However these codes require the knowledge of the structural characteristics of the blades that could be obtained through another identification process [4]. Therefore, the purpose of this chapter is to provide, therefore, the theoretical basis for such simulation codes.

2.1 ACTUATOR DISC MODEL

The behaviour of a wind turbine, at the beginning, can be simplified by taking into account only a steady and incompressible flow field and by disregarding the flow near the rotor disc. Basically this led to neglect the flow field near the rotor, which means to consider sudden variations of the fluid dynamic quantities in proximity of the disc itself. This physical situation can be modelled assuming a wind turbine as a discontinuous surface for the flow field.

When the airflow crosses the rotor disc, the wind turbine subtracts a part of its kinetic energy, so the wind slows down. Only the mass of air that passes through the rotor disc is involved, remaining separate from the air which passes outside the disc.

The affected air mass is contained within a boundary surface which extends from upstream to downstream forming a long stream tube of circular cross sections. The stream tube, by definition, is a surface whose particles of air move remaining confined into it. The flow of the airmass through the stream tube is null, since the particles of air cannot cross it.

Therefore, the mass flow rate of the air does not change in the boundary surface along the stream-wise direction and so

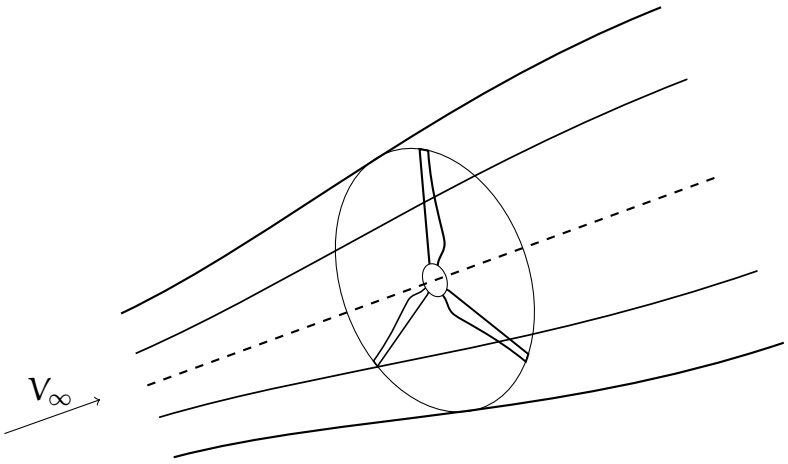

Figure 1: Wind turbine stream tube

the cross-sectional area of the stream tube must expand since the airflow slows down and does not become compressed as supposed. The enlargement of the stream tube when the airflow crosses the rotor disc during the operating conditions of a wind turbine is depicted in figure 1.

Before approaching the disc, the mass of air slows down and when it reaches the rotor disc has already a lower speed compared with the free stream wind speed. As a consequence, when the kinetic energy decreases, the static pressure increases, because no work is done on, or by, the mass of air.

When the air crosses the rotor disc and proceeds downstream, its static pressure decreases under the atmospheric pressure. Since the energy contained in the stream tube is different from the one that is contained outside, it is possible that a discontinuity contact develops downstream. This region is called the *wake*. At infinity downstream the environmental static pressure is restored at the expense of kinetic energy, thus the airflow slows down while the cross-sectional area of the stream tube continues to increase. The difference between the kinetic energy upstream and downstream corresponds to a power spent

by the airflow. For the principle of the conservation of energy this power cannot disappear but it is exactly the power captured by the wind turbine, up to losses due to other effects which are described in details below.

The first model, presented in the next section and based on the disc actuator theory, was developed by W.J.R. Rankine in the second half of nineteenth century.

2.2 MOMENTUM THEORY

The momentum theory represents a basic model which attempts to explain, in a simple way, the extraction of kinetic energy from the wind. This theory is very simple, but has some limitations because it does not describe exactly the behaviour of a wind turbine. Some of these neglected effects are considered in the models presented below. However, despite its simplicity, this model is always presented in the literature because it allows to obtain some useful information about a wind turbine.

It is important, firstly, to emphasize that this model solely takes into account only the process of extraction of energy. In fact in this section there is no connection with the geometry of the wind turbine, which, in this model, is simply replaced by a disc, called *actuator disc*.

This model assumes that the physical quantities within the stream tube are the same in every disc normal to the wind turbine axis. Basically this corresponds to consider average quantities inside every cross-section of the stream tube as it can be seen in figure 2, even though, actually, these quantities vary within the sections, for example when the corrections due to the finite number of blades are considered as explained below.

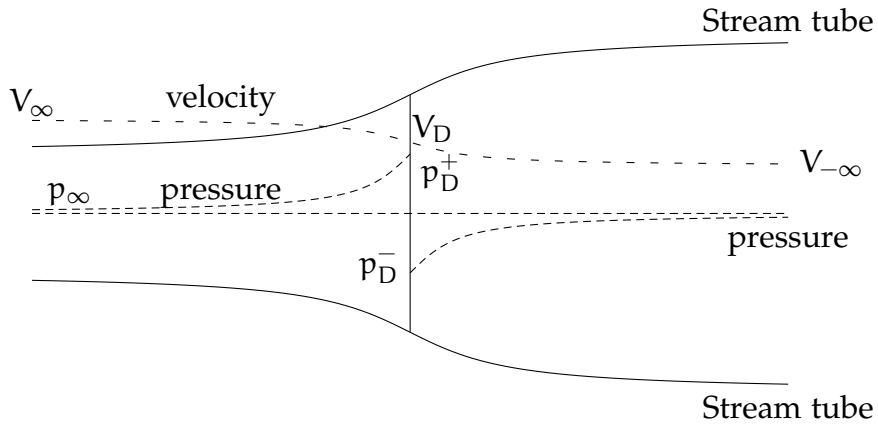

Figure 2: Actuator disc model

It is also assumed that the airflow velocity has only an axial, one-dimensional, component. As a result, this model neglects the rotational effects as well as the radial variation of velocity that causes the enlargement of the stream tube. Actually, these effects, always occur, but the momentum theory simply considers that these effects have a weak influence on the behaviour of a wind turbine.

The mass of air that passes through a cross section of the stream tube per unit time is $\rho A V$, where ρ is the air density, V is the wind speed and A is the cross-sectional area of the stream tube. Since the mass flow rate must be the same along the stream tube direction, from continuity equation it results

$$\dot{m} = \rho A_\infty V_\infty = \rho A_D V_D = \rho A_{-\infty} V_{-\infty}, \tag{2.1}$$

where $\infty, D, -\infty$ respectively refer to infinity upstream, on the disc and infinity downstream quantities.

The air which passes through the actuator disc, experiences a change in velocity, and also a rate of change of momentum equal to $(V_\infty - V_{-\infty})\rho A_D V_D$. This rate of change of momentum

can be induced only by the pressure drop $p_D^+ - p_D^-$ through the actuator disc surface, as depicted in figure 2. Hence

$$(p_D^+ - p_D^-)A_D = (V_\infty - V_{-\infty})\rho A_D V_D. \tag{2.2}$$

The first member of equation 2.2 can be valued applying Bernoulli's equation. As a consequence of the principle of conservation of energy, Bernoulli's equation states that the total energy, given by the contributions of kinetic, potential and the static pressure energy, remains constant, under steady conditions, if no work is done by, or on the air.

Since the energy is not conserved on the disc, Bernoulli's equation must be applied separately to the upstream and downstream sections of the stream tube. It follows

$$\begin{aligned} p_\infty + \frac{1}{2}\rho V_\infty^2 &= p_D^+ + \frac{1}{2}\rho V_D^2, \\ p_{-\infty} + \frac{1}{2}\rho V_{-\infty}^2 &= p_D^- + \frac{1}{2}\rho V_D^2, \end{aligned} \tag{2.3}$$

from which it results

$$p_D^+ - p_D^- = \frac{1}{2}\rho(V_\infty^2 - V_{-\infty}^2), \tag{2.4}$$

and finally, by equation 2.2,

$$\frac{1}{2}\rho A_D(V_\infty^2 - V_{-\infty}^2) = (V_\infty - V_{-\infty})\rho A_D V_D. \tag{2.5}$$

Introducing the so-called *axial interference factor* a, which represents the ratio of $V_\infty - V_D$ to V_∞, and is defined such that

$$V_D = V_\infty(1-a), \tag{2.6}$$

we obtain, from the equation 2.5,

$$V_{-\infty} = V_\infty(1-2a). \tag{2.7}$$

Thus the axial interference factor a far downstream is twice as the induction factor on the disc. Therefore the equation above

states that, to avoid the flow recirculation in the wake, the axial interference factor a cannot exceeds 0.5 because when this happens the velocity of the wind becomes negative and breaks the assumption of the actuator disc model which supposes only one dimensional flow velocity.

Anyway, flow recirculation does not actually occur because the wake becomes turbulent and a part of the air enters from outside the wake.

The equation 2.2, using the axial interference factor, becomes

$$F = 2\rho A_D V_\infty^2 a(1-a), \tag{2.8}$$

while the power extracted by the actuator disc is

$$P = FV_D = 2\rho A_D V_\infty^3 a(1-a)^2. \tag{2.9}$$

The power available in the wind, at given velocity, in absence of the wind turbine, is related to the kinetic energy of the particles and it is given by

$$P_{ref} = \frac{1}{2}\dot{m}V_\infty^2 = \frac{1}{2}\rho A_D V_\infty^3. \tag{2.10}$$

A useful dimensionless quantity, defined as the ratio of the net extracted power by the wind turbine to the total energy, P_{ref}, available in the air is the *power coefficient*,

$$C_P = \frac{2\rho A_D V_\infty^3 a(1-a)^2}{\frac{1}{2}\rho A_D V_\infty^3} = 4a(1-a)^2. \tag{2.11}$$

Similarly it is possible to introduce the *thrust coefficient* as

$$C_T = \frac{T}{\frac{1}{2}\rho A_D V_\infty^2} = 4a(1-a). \tag{2.12}$$

Finally a *torque coefficient* related to the torque that the air exerts on a wind turbine can be defined by

$$C_Q = \frac{Q}{\frac{1}{2}\rho A_D V_\infty^2 R}. \tag{2.13}$$

The thrust and the power coefficients are considered the fundamental operating characteristics for a wind turbine.

Being the power coefficient a function of the axial interference factor, it is possible to solve equation 2.11 in order to obtain the maximum of the power coefficient setting $\frac{d}{da}C_p = 0$. It can easily be seen that the maximum is achieved for $a = 1/3$ which gives

$$C_{p_{max}} = \frac{16}{27} \approx 0.593. \tag{2.14}$$

This is the maximum value of the power coefficient achievable within the momentum theory. It is called the *Betz limit* and it is a fundamental result of momentum equation. Up to now, no wind turbine has exceeded this limit, without introducing some variations in the structure of the turbine. The Betz limit can only be overcome by a shrouded wind turbine for which, of course, momentum theory cannot apply.

It is important to underline that the Betz limit does not depend on the ability of designing a wind turbine, but it depends on the model itself because the cross sectional area of the stream tube infinity upstream is smaller than the area of the actuator disc, as it can be seen in figure 1. Practically it is like the net area involved in the process is less than the area of the rotor disc. The mere presence of the wind turbine implies that only a part of all the energy available in the wind can be converted into electrical energy.

2.3 GENERAL MOMENTUM THEORY

The theory developed until now supposes only axial variation of the velocity. The real process of extraction of energy for a

wind turbine is obtained through a number of blades which rotate around an axis. The blades develop a pressure difference across the rotor disc and produce the loss of momentum downstream. The air exerts a torque on the rotor disc which, by Newton's third low, also exerts a torque on the air. Since this torque necessarily involves a rotation of the airflow, a model that considers this effects is needed.

The model that takes into account these rotational effects is called *general momentum theory*. This theory supposes that the physical quantities, for example the tangential velocities that the airfoils sections see, vary in the radial direction. In order to account for these variations the model divides the whole disc in several annular regions. It is also assumed that these infinitesimal rings operate without interacting with the other annuli. Therefore the variation of momentum is considered separately in each ring.

The torque of the annular region of radius r is equal to the rate of change of angular momentum of the air

$$dQ = \omega r^2 \, d\dot{m} = 4\pi r^3 \rho V_D (1 - a) \Omega a' \, dr. \tag{2.15}$$

The symbol Ω represents the angular velocity of the wind turbine while ω is the angular velocity acquired in the wake by the air. Finally a', called *tangential interference factor*, is a quantity related to the rotational velocity of the particles. It is defined as

$$a' = \frac{\omega}{2\Omega}, \tag{2.16}$$

and it causes a further loss of kinetic energy that could be extracted by the wind turbine.

It is important to specify that upstream the air does not experience any rotational velocity. The rotational velocity $2\Omega r a'$ is acquired completely along the thickness of the rotor disc.

An expression for the thrust can be similarly derived and it is given by [11, 19]

$$dT = 4\pi\rho V_\infty^2 (1-a) a r \, dr. \tag{2.17}$$

2.4 BLADE ELEMENT THEORY

Until now there is no reference to the blades in the process of extraction of energy. But it is clear that the rate of change of axial and angular momentum of air which passes through the actuator disc is a consequence of the aerodynamic forces that act along the blades. The theory which makes possible the evaluation of the forces acting on the blades of a wind turbine is the so called *blade element theory*.

This theory, like general momentum theory, assumes that the blades can be divided into several elements that act independently from each other. Furthermore blade element theory supposes that the flow, interacting with the blade elements, has only two-dimensional component.

Such a situation allows to consider two-dimensional aerodynamic characteristics of the airfoils, namely lift and drag coefficients, using the angle of attack that results from the composition of axial and tangential velocities in the plane of the airfoils. These 2D lift and drag coefficients can be obtained through experimental measurements made in wind tunnels or through simulation codes like XFOIL [5]

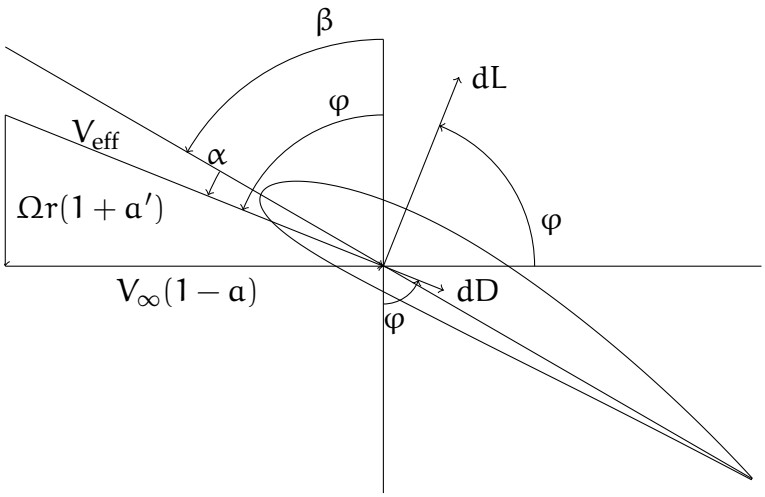

Figure 3: Blade element operating condition

In this way it is very simple to calculate the forces that act on the blades. However this theory continues to neglect the radial flow and three-dimensional effects, for example stall delay.

One of the goals of this thesis work is actually the inclusion of such effects by an adequate set of airfoils characteristics table. To date,except for CFD that has its limitations and it is computationally too much onerous to be considered, there are no models that include such effects.

The velocity that an element of the blade sees, at a distance r from the axis of the wind turbine, is the composition of the axial velocity, given by $V_\infty(1-a)$, due to the slowdown of the wind, and tangential velocity which can be written as $\Omega r(1+a')$, due to the rotational effects.

Therefore the total velocity that acts on the blade element at distance r from the axis is given by

$$V_{\mathit{eff}} = \sqrt{\left(V_\infty(1-a)\right)^2 + \left(\Omega r(1+a')\right)^2}. \tag{2.18}$$

Figure 3 shows the composition of the velocities in the plane of the airfoil and the forces acting on the latter.

The angle φ, called *inflow angle*, has great importance because it allows to calculate the torque and the thrust on the blades starting from the aerodynamic forces on the airfoils. The angle φ is defined by (see figure 3)

$$\tan\varphi = \frac{V_\infty(1-a)}{\Omega r(1+a')} = \frac{1}{\chi}\frac{1-a}{(1+a')}. \tag{2.19}$$

The angle of attack α that the airfoil sees is given by $\varphi - \beta$ where β represents the pitch angle.

The quantity χ that appears in equation 2.19 is called *local speed ratio* and it is defined as

$$\chi = \frac{\Omega r}{V_\infty}. \tag{2.20}$$

The local speed ratio related to the radius of the wind turbine, i.e. $r = R$, is a quantity of great importance. It is the ratio between the rotational velocity that the tip of the blade sees and the velocity of the wind far upstream. It is called *tip speed ratio* and it denoted by

$$\lambda = \frac{\Omega R}{V_\infty}. \tag{2.21}$$

The importance of the tip speed ratio is highlighted by the fact that the fundamental characteristics curves, namely C_P and C_Q, for a wind turbine are defined as a function of the tip speed ratio itself. These curves, moreover, are not independent but are related by $C_P = \lambda C_Q$. So the knowledge of only one of these quantities is fundamental because the other can be acquired from the equation above.

The lift force that acts on the blade element is

$$dL = \frac{1}{2}\rho V_{eff}^2 c C_l \, dr, \tag{2.22}$$

while the drag can be written as

$$dD = \frac{1}{2}\rho V_{eff}^2 c C_d \, dr. \tag{2.23}$$

If the dependence of C_l and C_d from α is known, together with the interference factors, then it is possible to calculate the forces acting on the element of the blade. Therefore, the total forces that act on a blade are obtained integrating along the blade span and the total force acting on the wind turbine can be determined by multiplying the total force for the number of the blades.

2.5 THE BLADE ELEMENT MOMENTUM THEORY

The *blade element momentum theory* represents one of the most important models for performance prediction of wind turbines. In fac,t it is widely used by industry for a preliminary analysis of wind turbines design mainly for its simplicity, low computational efforts and finally for its good degree of reliability.

This theory, developed by Glauert and Betz, combines both momentum theory and the blade element theory, on an annulus of radius r. It allows calculating induced velocities and loads on the elements of the blades and, consequently, to predict the performance of the wind turbines.

The component of the aerodynamic force in the axial direction that acts on N blade elements is

$$dT = dL\cos\varphi + dD\sin\varphi = \frac{1}{2}\rho V_{eff}^2 Nc(C_l\cos\varphi + C_d\sin\varphi)\,dr. \tag{2.24}$$

Similarly, the overall torque that acts on N blade elements of the wind turbine is given by

$$dQ = r\sin\varphi\,dL - r\cos\varphi\,dD = \frac{1}{2}\rho V_{eff}^2 Nc(C_l\sin\varphi - C_d\cos\varphi)r\,dr. \tag{2.25}$$

Since the blade element momentum theory supposes that the loss of momentum of the air is due to the aerodynamic forces, i.e. lift and drag, that act on the blade elements, equating the expressions in the equations 2.17 and 2.24 for the thrust, and in the equations 2.15 and 2.25 for the torque, it results

$$\begin{aligned} \frac{a}{1-a} &= \left(\frac{\sigma R}{8r}\right)\left(\frac{C_l \cos\varphi + C_d \sin\varphi}{\sin^2\varphi}\right), \\ \frac{a'}{1+a'} &= \left(\frac{\sigma R}{8r}\right)\left(\frac{C_l \sin\varphi - C_d \cos\varphi}{\sin\varphi\cos\varphi}\right), \end{aligned} \tag{2.26}$$

where σ is called *local blade solidity* and it is related to the ratio between the total chord length at a distance r from the axis and the length of the circumference of radius r, i.e.

$$\sigma = \frac{Nc}{2\pi r}. \tag{2.27}$$

These equations can be iteratively solved to found the interference factors and the aerodynamic forces that act on the blade elements. Therefore, the overall performance of the given wind turbine can be calculated.

2.6 LIMITS OF THE BLADE ELEMENT MOMENTUM

The blade element momentum theory, as pointed out above, is often used to predict the behaviour of a wind turbine. However it continues to neglect some physical phenomena related to the operating conditions of a wind turbine. This fact is due mainly to the assumptions that simplify the model, which results from the need of reducing the computational efforts, in order to follow the principle of parsimony. But the fundamental reason is due to the impossibility of accurately describing the real behaviour of a wind turbine through the actual theoretical knowledge of the aerodynamic laws. For this reason the model

does not consider how the process really develops, but it only provides an approximation of the real behaviour of the wind turbine. The major limitations of the blade element momentum theory are listed below:

- the evaluation of the performance is possible only during steady wind conditions;
- the effects of the radial flow, namely three-dimensional effects, are neglected because the model assumes that the blade elements act independently from each other;
- the effects of the deflections of the blades, namely aeroelastic effects, that always occur due to the aerodynamic forces, are not taken into account by the model.

On the other hand it is possible to include some corrections related to other limitations that have not been described in the theory, to increase the fidelity of the model with the real process. For example it is possible to take into account for the discrete number of blades, as exhibited in the next section.

2.7 TIP AND ROOT LOSSES

The blade element momentum theory supposes that the wind turbine has a great number of blades such that every particle in the air interacts with someone of them. A wind turbine has generally three blades because this configuration guarantees the best compromise in order to obtain the maximum amount of energy from the wind. There also exist wind turbines with different number of blades. Due to the finite number of blades a great number of particles passes through the disc rotor interacting with any blade. Consequently the wind turbine experi-

ences a reduction in torque, and in power as well. In particular the axial interference factor vary within every annular. In fact it is greater when it is near the blade element, while it decreases otherwise. The overall loss of momentum in the blade element momentum theory is established by the average value of the interference factor. But when the interference factor a is greater, namely near the blade elements, the inflow angle φ is smaller. So the contribution of the lift force on the rotor plane is reduced and it determines a smaller amount of torque. Since this phenomenon is evident especially near the tip, it is called *tip-losses*.

The general problem, that takes into account this losses, was solved by Goldstein, but it is difficult to deal with. For this reason a simplified model, proposed by Prandtl, and adopted by the simulation codes used in this work, is generally preferred. The result of this model, which is used by many simulation codes, allows to define a corrective function for the axial interference factor, whose analytic form is given below

$$F_{tip} = \frac{2}{\pi} \arccos(\exp(-f_{tip})), \tag{2.28}$$

where f_{tip} is given by

$$f_{tip}(r) = \frac{N}{2} \frac{(1 - r/R)}{(r/R) \sin \varphi}. \tag{2.29}$$

Similarly, Prandtl introduced a model that takes into account the so-called *root-losses*. The corrective function related to this losses is defined by

$$F_{hub} = \frac{2}{\pi} \arccos(\exp(-f_{hub})), \tag{2.30}$$

where f_{hub} is given by

$$f_{hub}(r) = \frac{N}{2} \frac{(r/R - r_{hub}/R)}{(r_{hub}/R) \sin \varphi}. \tag{2.31}$$

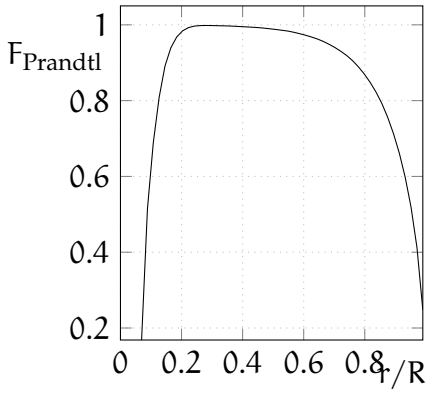

Figure 4: Prandtl tip-root losses factor

The analytic expression of the overall corrective factor is given by $F_{Prandtl} = F_{tip} \cdot F_{hub}$ while a graphical representation of this function can be seen in figure 4.

Finally, the corrective function $F_{Prandtl}$ of Prandtl enters in the equations 2.26 in the following manner

$$\begin{aligned} \frac{a}{1-a} &= \left(\frac{\sigma R}{8 r F_{Prandtl}}\right)\left(\frac{C_l \cos\varphi + C_d \sin\varphi}{\sin^2\varphi}\right), \\ \frac{a'}{1+a'} &= \left(\frac{\sigma R}{8 r F_{Prandtl}}\right)\left(\frac{C_l \sin\varphi - C_d \cos\varphi}{\sin\varphi\cos\varphi}\right). \end{aligned} \tag{2.32}$$

2.8 VITERNA CORRIGAN MODEL

Under operating conditions of a wind turbine, the airfoils sections, placed along the blades, work at wide ranges of angles of attack. Since experimental measurements or simulation codes can provide in a reliable way the characteristics of airfoils only for lower angles of attack, the properties at high angles of attack are generally unavailable. Therefore a method that allows to obtain the aerodynamic characteristics related to higher angles of attack is needed.

A semi-empirical model that attempts to describe the post-stall region was proposed by Viterna and Corrigan [20, 21]. It

will be used during the identification of the aerodynamic properties in order to obtain the aerodynamic characteristics related to high angles of attach that are very difficult to identify in a direct way.

This model was validated by several experimental results [12–14] performed on some wind turbines. It supposes that the airfoil at high angles of attack has characteristics that are similar to those of flat plate. Hence, the properties of the airfoils at high angles of attack are described by the following relations

$$C_l(\alpha) = A_1 \sin(2\alpha) + A_2 \frac{\cos^2(\alpha)}{\sin(\alpha)}, \tag{2.33}$$

$$C_d(\alpha) = B_1 \sin^2(\alpha) + B_2 \cos(\alpha), \tag{2.34}$$

where the constant values A_1 and B_1 can be calculated as follow

$$B_1 = C_{dmax}, \tag{2.35}$$

$$A_1 = \frac{C_{dmax}}{2}. \tag{2.36}$$

The maximum drag coefficient can be calculated through the expression given below, based on experimental measurement [6] for $AR \leqslant 50$

$$C_{dmax} = 1.11 + 0.018AR. \tag{2.37}$$

Solving the equations 2.33 and 2.34 with respect to A_2 and B_2 using 2.35 and 2.36 it results

$$A_2 = \left(C_l - C_{dmax} \sin(\alpha)\cos(\alpha)\right) \frac{\sin(\alpha)}{\cos^2(\alpha)}, \tag{2.38}$$

$$B_2 = \frac{C_d - C_{dmax} \sin^2(\alpha)}{\cos(\alpha)}, \tag{2.39}$$

so, given the continuity of the properties of airfoils at α_s, that is the stall angle, it results

$$A_2 = \left(C_{ls} - C_{dmax} \sin(\alpha_s)\cos(\alpha_s)\right) \frac{\sin(\alpha_s)}{\cos^2(\alpha_s)}, \tag{2.40}$$

$$B_2 = \frac{C_{ds} - C_{dmax} \sin^2(\alpha_s)}{\cos(\alpha_s)}, \tag{2.41}$$

where C_{ls} and C_{ds} are related to the lift and drag properties of the airfoils at stall angle of attack. The angle α_s used in these equations can differ from the real stall angle and in general it is the higher angle at which the aerodynamic properties are available.

3

SYSTEM IDENTIFICATION THEORY

3.1 INTRODUCTION

In this chapter the required theory about system identification is presented [8–10] for the development of the thesis work, together with some methods for practical applications. This theory will be applied to wind turbines in chapter 4, which regards the identification of the aerodynamic characteristics of wind turbines. These methods could also be used for the identification of the structural properties of wind turbines as it has been done in [4].

The theory of system identification is concerned with the determination of an adequate mathematical model for a physical system given the input and the output measurement and the behaviour of the physical system itself.

A definition of *system identification*, proposed by Zadeh [22], is reported below.

System identification is the determination, on the basis of observation of input and output, of a system within a specified class of systems to which the system under test is equivalent.

The definition given above means that several mathematical models of a dynamical system can exist. The choice among all these models must be made following the *principle of parsimony*. These principles states that, among all the different models, the simplest one must be chosen. This model must however be able

to describe the phenomenon with the required degree of approximation. The most comprehensive models are not always the best models because they very often require great computational efforts and, because generally, the greater number of parameters they have the more it can sometime lead to convergence troubles, as experience has shown and as it can be seen with an example in chapter 4 during the identification of wind turbines.

Another characteristic of system identification is that it is based on experimental data, which are always affected by noise. For this reason a statistical approach, as detailed below, must be considered in order to account for these errors.

Finally a method must be introduced in order to establish the equivalence between a model within the class of all models and the real physical dynamic system considered. Since this equivalence can be described for simplicity by a scalar function that correlates the output of the real system to those produced by the mathematical model, the problem of system identification can be reduced to an optimization problem.

3.2 MATHEMATICAL MODELING

The first fundamental step that must be considered in addressing the problem of system identification is the formulation of an adequate model that represents the physical system. There exist two different ways to create a mathematical model for a physical process.

The *behavioural models* are used when it is impossible to derive a theoretical model for the physical system in an adequate way or when, even if it is possible, it requires huge compu-

tational efforts and therefore, it cannot be used in reasonable times. These models are called black-box because they are solely based on input and output data reproducing the system response without any knowledge of the behaviour of the process. Therefore, the parameters of such these models have no physical meaning.

The other way used to obtain a model for a dynamic system is represented by *phenomenological models*. These representations are obtained through a rigorous theoretical formulation of the physical process. The behaviour of the system and the relations between input and output quantities are derived considering the physic underlying the process and its related laws. In this case the parameters have almost always a physical interpretation and it is possible to limit such parameters within certain ranges in the optimization problem.

The mathematical formulation of the model for a wind turbine is derived in chapter 2. It uses precisely such a description because it derives the behaviour of wind turbines using aerodynamic laws.

3.3 PARAMETER ESTIMATION

The goal of system identification theory is the determination of a model, within a wide class of models, that better represents the physical system being investigated. Usually the models used to represent the physical system have the same mathematical structure since they are generally derived from the same formulation. This means that all the models, belonging to the same class, have the same mathematical form and they differ only for the values assumed by the *parameters* of the model

structure. Furthermore since the equivalence between the physical system and the mathematical models can be established by the value of a function, called *cost function*, the problem of parameter estimation can be reduced to an optimization problem.

The set of models can be written as

$$\mathfrak{M} = \{\mathfrak{M}(\theta) | \theta \in D_{\mathfrak{M}}\}, \tag{3.42}$$

where $\theta \in \mathbb{R}^n$ is the column vector of parameters.

Let $y = h(\theta) \in \mathbb{R}^m$ be the m-dimensional column vector of *model output*.

A model is called *linear* if the model output $y = h(\theta)$ is a linear function of the parameters. If the model output is not a linear function of the parameters the model is called *nonlinear*.

Now let $Z_N = \{z_1, \ldots, z_N\}$ be the set of N experimental m-dimensional measurements, i.e. $z_i \in \mathbb{R}^m$. The relation between y and z is given by

$$z = y + v, \tag{3.43}$$

where v is the *measurement error*.

Under these assumptions the optimization problem can be solved by finding the vector of parameters θ that minimizes the scalar cost function

$$J = J(Z_N, y, \theta). \tag{3.44}$$

The cost function depends obviously on the parameters, but it also depends on the choice of the model structure for the physical system too. Finally, the cost function depends on the experimental measurements obtained.

Since the optimization problem is generally performed once the model structure and the experimental measurements are

established, the cost function can be assumed to depend only on the vector of the parameters θ. Therefore

$$J = J(\theta). \tag{3.45}$$

Usually the cost function is defined through the differences between the experimental measurement z and the output y of the assumed model since the identified model is the model capable of reproducing the responses of the physical system as better as possible. Various forms for the cost function are presented in the next sections. They depend on the chosen model for the uncertainties in the parameters and measurements.

3.3.1 *Estimator for the Least-Squares model*

The estimator for the least squares model is the simplest estimator model and it requires no uncertainty model for the vector of parameters θ and the measurement noise $\nu = z - h(\theta)$. It is obtained, as highlighted earlier, observing that the best estimate for θ is the estimate that minimizes the difference between the experimental measurements and the output of the assumed model. In particular the least squares model minimizes the following weighted sum

$$J(\theta) = \frac{1}{2}\nu^T R^{-1}\nu, \tag{3.46}$$

with R^{-1} a positive definite matrix used to weight the several output data in order to give different importance to the different output measurements.

Therefore the *ordinary least squares* estimator is obtained if R is chosen as the identity matrix. The relative cost function is

$$J(\theta) = \frac{1}{2}\nu^T\nu.$$

Considering that there can also be several experimental measurements, namely N, the cost functions in the two cases become

$$J(\theta) = \frac{1}{2}\sum_{i=1}^{N}\nu_i^T R^{-1}\nu_i, \tag{3.47}$$

$$J(\theta) = \frac{1}{2}\sum_{i=1}^{N}\nu_i^T\nu_i. \tag{3.48}$$

3.3.2 *Estimator for the Fisher model*

The estimator for the Fisher model is based on the Fisher estimation theory. In order to identify the unknown parameters it uses the *likelihood function*

$$\mathbb{L}(Z_N, \theta) = \mathbb{P}(Z_N|\theta), \tag{3.49}$$

where $\mathbb{P}(Z_N|\theta)$ is the conditional probability of the measurements Z_N, given the vector of parameters θ. The maximum likelihood estimator is the most common estimator for the Fisher model. It maximizes the conditional probability $\mathbb{L}(Z_N, \theta)$, i.e. it finds the vector of parameters θ in correspondence of which the experimental measurements have the maximum probabil-

ity to be realized. The likelihood function could be also written, applying the properties of conditional probability, as

$$\begin{aligned}\mathbb{L}(Z_N, \theta) &= \mathbb{L}(z_1, \ldots, z_N, \theta) \\ &= \mathbb{L}(z_N | Z_{N-1}, \theta)\mathbb{L}(Z_{N-1}, \theta) \\ &\vdots \\ &= \prod_{i=1}^{N} \mathbb{L}(z_i | Z_{i-1}, \theta).\end{aligned} \tag{3.50}$$

If the measurements z_i are independent from each other and the measurement noise ν_i is normally distributed with zero mean, it follows

$$\begin{aligned}\mathbb{L}(z_i | Z_{i-1}, \theta) &= \mathbb{L}(z_i) \\ &= \left((2\pi)^m |R|\right)^{-1/2} \exp\left[-\frac{1}{2}\nu_i^T R^{-1} \nu_i\right],\end{aligned} \tag{3.51}$$

where R is the measurement error covariance matrix. Assuming that the measurement noises are independent from each other, it results

$$\mathbb{E}(\nu_i \nu_j^T) = R \cdot \delta_{ij}. \tag{3.52}$$

The likelihood function can be finally written as

$$\mathbb{L}(Z_N, \theta) = \prod_{i=1}^{N} \left((2\pi)^m |R|\right)^{-1/2} \exp\left[-\frac{1}{2}\nu_i^T R^{-1} \nu_i\right]. \tag{3.53}$$

The maximization of the likelihood function in equation 3.53 can be equivalently solved by minimizing the negative logarithm of the likelihood function itself in order to simplify the optimization problem since the probability density in equation 3.53 contains an exponential function. This method is possible because the logarithm is a monotonic function and it transforms an extreme point into an extreme point.

The cost function J to be minimized is therefore

$$\begin{aligned} J &= -\ln \mathbb{L}(Z_N, \theta) \\ &= \frac{1}{2}\sum_{i=1}^{N} \nu_i^T R^{-1} \nu_i + \frac{N}{2}\ln|R| + \frac{Nm}{2}\ln(2\pi). \end{aligned} \tag{3.54}$$

Once the experimental measurements and the number of output are known, the last term is constant and, since it does not enter in the optimization process, the cost function J can be finally written as

$$J = \frac{1}{2}\sum_{i=1}^{N} \nu_i^T R^{-1} \nu_i + \frac{N}{2}\ln|R|. \tag{3.55}$$

If R is a constant matrix, neglecting the last constant term in equation 3.55, the function J becomes

$$J = \frac{1}{2}\sum_{i=1}^{N} \nu_i^T R^{-1} \nu_i,$$

that is exactly the cost function of the least squares model.

3.3.3 *Estimator for the Bayesian model*

The estimator for the Bayesian model uses the Bayesian estimation theory. It requires that the probability density of the parameters and the measurement noise are known a priori. These informations allow, by the Bayes's rule, to obtain the a posteriori probability for the parameters. This model is scarcely used due to the difficulties connected with the strong assumption on the a priori probability of the parameters, nevertheless the results of this model are reported for completeness.

An estimator for the Bayesian model could be the one that maximizes this conditional probability that, by the Bayes's rule, assumes the following form

$$\mathbb{P}(\theta|z) = \frac{\mathbb{P}(z|\theta)\mathbb{P}(\theta)}{\mathbb{P}(z)}. \tag{3.56}$$

If θ is supposed to be $N(\theta_p, \Sigma)$ and $\nu \in N(0, R)$, then

$$\mathbb{P}(\theta) = \left((2\pi)^m|\Sigma|\right)^{-1/2} \exp\left[-\frac{1}{2}(\theta-\theta_p)^T\Sigma^{-1}(\theta-\theta_p)\right], \quad (3.57)$$

while the conditional probability $\mathbb{P}(z|\theta)$ can be written as

$$\mathbb{P}(z|\theta) = \left((2\pi)^N|R|\right)^{-1/2} \exp\left[-\frac{1}{2}\nu^T R^{-1}\nu\right]. \quad (3.58)$$

Substituting these expressions in equation 3.56 it follows

$$\mathbb{P}(\theta|z) = \frac{\left((2\pi)^{N+m}|R||\Sigma|\right)^{\frac{1}{2}} \exp\left[-\frac{\left(\nu^T R^{-1}\nu+(\theta-\theta_p)^T\Sigma^{-1}(\theta-\theta_p)\right)}{2}\right]}{\mathbb{P}(z)}.$$

Using the negative logarithm, as it has been done for the Fisher model, and observing that the probability $\mathbb{P}(z)$ has no effects on the optimization process, since it does not depend on θ, the cost function J can be finally written as

$$J = \frac{1}{2}\left(\nu^T R^{-1}\nu + (\theta-\theta_p)^T\Sigma^{-1}(\theta-\theta_p)\right). \quad (3.59)$$

3.4 COST FUNCTION OPTIMIZATION ALGORITHM

In this section some methods, which can be used for the minimization of the cost function of the maximum likelihood estimator [8, 9], will be presented.

3.4.1 *Relaxation strategy*

The optimization of the cost function, that is recalled below

$$J(\theta) = \frac{1}{2}\sum_{i=1}^{N} \nu_i^T R^{-1}\nu_i + \frac{N}{2}\ln|R|,$$

can be realized using the so-called *relaxation strategy*. Since both R and θ are unknown, the basic idea of this method is that the

optimization problem can be simplified if the unknowns are identified alternately, keeping fixed the other. Therefore, this technique divides the optimization problem into two steps.

In the first step the cost function is minimized with respect to R. Differentiating with respect to the matrix R and setting the resulting equation to zero, an estimation for the covariance matrix is obtained as follow (see [8, 9])

$$R = \frac{1}{N} \sum_{i=1}^{N} \nu_i^T \nu_i. \tag{3.60}$$

In the second step, given this expression for the covariance matrix R, the cost function can be solved with respect to the vector of parameters, keeping the matrix R fixed. The cost function assumes now the following form

$$J(\theta) = \frac{1}{2} \sum_{i=1}^{N} \nu_i^T R^{-1} \nu_i, \tag{3.61}$$

and it can be optimized to obtain a vector of parameters θ.

With this updated vector of parameters, a new covariance matrix can be calculated and another optimization problem can be performed to obtain an improved vector of parameters. Therefore these two steps are repeated until the criteria for the convergence of the parameters are satisfied.

A mathematical proof for this relaxation strategy does not exist. Anyway this method is widely used in practice and several tests have also provided results with good degree of reliability.

3.4.2 *Gauss-Newton method*

This section is concerned with the optimization of the function in equation 3.61. The approach presented below for the

optimization process is based on the *Newton-Raphson method*. It starts with the necessary condition for extreme points, that is

$$\frac{\partial J(\theta)}{\partial \theta} = 0. \tag{3.62}$$

The first order Taylor series expansion of the gradient function can be written as

$$\frac{\partial J}{\partial \theta}(\theta_0 + \Delta\theta) \approx \frac{\partial J}{\partial \theta}(\theta_0) + \left.\frac{\partial^2 J}{\partial \theta^2}\right|_{\theta=\theta_0} \Delta\theta, \tag{3.63}$$

where $\Delta\theta$ represents the vector of change of the parameter, $\partial J/\partial\theta$ the gradient of the cost function, and $\partial^2 J/\partial\theta^2$ the Hessian matrix, i.e. the second order gradient matrix.

Using the necessary condition, the expression in equation 3.63 can be matched to zero and it can be solved in order to find the parameter change $\Delta\theta$. It results

$$\Delta\theta = -\left(\left.\frac{\partial^2 J}{\partial \theta^2}\right|_{\theta=\theta_0}\right)^{-1} \frac{\partial J}{\partial \theta}(\theta_0). \tag{3.64}$$

Calculating the gradient function it follows

$$\frac{\partial J}{\partial \theta} = -\sum_{i=1}^{N} \left[\frac{\partial y_i}{\partial \theta}\right]^T R^{-1}(z_i - y_i), \tag{3.65}$$

while the calculation of the Hessian matrix leads to

$$\frac{\partial^2 J}{\partial \theta^2} = \sum_{i=1}^{N} \left[\frac{\partial y_i}{\partial \theta}\right]^T R^{-1} \frac{\partial y_i}{\partial \theta} + \sum_{i=1}^{N} \left[\frac{\partial^2 y_i}{\partial \theta^2}\right]^T R^{-1}(z_i - y_i). \tag{3.66}$$

The second term on the right-side of this last equation is very hard to calculate, due to the presence of the second gradient of the response, which requires a lot of computational efforts. However this term contains the factor $(z_i - y_i)$ that should go to zero when the process is going to converge. In assumption of

zero mean for the measurement noise, the contribution of the last term in equation 3.66 should disappear. This consideration can be exploited neglecting the term in question to simplify the calculation of the Hessian matrix. Therefore the following approximation for the Hessian matrix can be used

$$\frac{\partial^2 J}{\partial \theta^2} \approx \sum_{i=1}^{N} \left[\frac{\partial y_i}{\partial \theta}\right]^T R^{-1} \frac{\partial y_i}{\partial \theta}. \tag{3.67}$$

This simplified algorithm is called *modified Newton-Raphson* or *Gauss-Newton method*.

3.4.3 *Method of quasi-linearization*

In this section another method will be presented in order to find the vector of parameter change $\Delta\theta$. This method, called *quasi-linearization*, is still based on the necessary condition, but it works on the expression y of the output model. Calculating the gradient of the cost function it results

$$\frac{\partial J}{\partial \theta} = -\sum_{i=1}^{N} \left[\frac{\partial y_i}{\partial \theta}\right]^T R^{-1}(z_i - y_i) = 0. \tag{3.68}$$

Now, applying the first order expansion, this time to the output y_i instead of the gradient function, it results

$$y(\theta) = y(\theta_0 + \Delta\theta) \approx y(\theta_0) + \frac{\partial y}{\partial \theta}\Delta\theta. \tag{3.69}$$

If the linearized expression of the model output y is substituted in equation 3.68 as follows

$$\frac{\partial J}{\partial \theta} = -\sum_{i=1}^{N} \left[\frac{\partial y_i}{\partial \theta}\right]^T R^{-1}\left(z_i - y_i - \frac{\partial y_i}{\partial \theta}\Delta\theta\right) = 0. \tag{3.70}$$

Rearranging this equation in a more useful way leads to

$$\sum_{i=1}^{N}\left[\frac{\partial y_i}{\partial \theta}\right]^T R^{-1}\frac{\partial y_i}{\partial \theta}\Delta\theta = \sum_{i=1}^{N}\left[\frac{\partial y_i}{\partial \theta}\right]^T R^{-1}(z_i - y_i), \tag{3.71}$$

and the parameter change can be finally written as

$$\Delta\theta = -\mathcal{F}^{-1}\mathcal{G}, \tag{3.72}$$

where

$$\mathcal{F} = \sum_{i=1}^{N}\left[\frac{\partial y_i}{\partial \theta}\right]^T R^{-1}\frac{\partial y_i}{\partial \theta}, \tag{3.73}$$

$$\mathcal{G} = -\sum_{i=1}^{N}\left[\frac{\partial y_i}{\partial \theta}\right]^T R^{-1}(z_i - y_i). \tag{3.74}$$

The matrix $\mathcal{F}$ is also called *Fisher information matrix* while the elements of the matrix $G_i = \partial y_i/\partial\theta$ that appear in these equation are called *output sensitivities*.

Note that the parameter change in equation 3.72 is exactly the same obtained with the Gauss-Newton method in equation 3.64, once the Hessian matrix and the gradient of the cost function are explicitly calculated.

3.5 PROPERTIES OF THE ESTIMATES

In this section, the main properties of the parameters estimates obtained through the use of the maximum likelihood principle [8, 9] will be shown.

- The maximum likelihood estimates $\hat{\theta}_{ML}$ are asymptotically unbiased, i.e.

  $$\lim_{N\to\infty} \mathbb{E}(\hat{\theta}_{ML}) = \theta, \tag{3.75}$$

  where θ is the true, but unknown vector of parameters.

- The maximum likelihood estimates $\hat{\theta}_{ML}$ are asymptotically consistent, i.e.

$$\hat{\theta}_{ML} \xrightarrow{N\to\infty} \theta. \tag{3.76}$$

- The maximum likelihood estimates $\hat{\theta}_{ML}$ are asymptotically normally distribuited, i.e.

$$\hat{\theta}_{ML} \to N(\theta, \mathcal{F}^{-1}), \tag{3.77}$$

where $\mathcal{F}$ is the Fisher information matrix already seen in equation 3.73 and that is defined by

$$\mathcal{F} := \mathbb{E}\left[\left(\frac{\partial \ln \mathbb{L}}{\partial \theta}\right)\left(\frac{\partial \ln \mathbb{L}}{\partial \theta}\right)^T\right] = -\mathbb{E}\left(\frac{\partial^2 \ln \mathbb{L}}{\partial \theta^2}\right). \tag{3.78}$$

The first equality is a definition, while the proof of the second can be found in [9].

- The maximum likelihood estimates $\hat{\theta}_{ML}$ are asymptotically efficient, i.e.

$$\mathrm{Cov}(\hat{\theta}_{ML}) = \mathbb{E}\left[(\hat{\theta}-\theta)(\hat{\theta}-\theta)^T\right] \xrightarrow{N\to\infty} \mathcal{F}^{-1}. \tag{3.79}$$

The matrix $\mathcal{F}^{-1}$ is known as the Cramér-Rao lower bound. This name derives from the so called *Cramér-Rao inequality* that holds for an unbiased estimator $\hat{\theta}$ and which is reported below

$$\mathrm{Cov}(\hat{\theta}) \geqslant \mathcal{F}^{-1}. \tag{3.80}$$

Since the maximum likelihood estimates are asymptotically efficient, the main diagonal elements of the inverse of the Fisher information matrix allow to provide the lower bounds on the variance of the parameters, called *Cramér-Rao bounds*.

Therefore the accuracy for the estimated parameters can be evaluated by the diagonal elements of $\mathcal{F}^{-1}$. If the number of experimental measurements increases, the lower bounds can better estimate the variance of the parameters.

3.6 DETECTION OF DATA COLLINEARITY

A very important issue that must be considered in order to resolve the system identification problem, and in particular the identification of the aerodynamic characteristics of wind turbines, is *data collinearity*.

Data collinearity occurs when a parameter can be written as a linear combination of another or more parameters. If this circumstance occurs, the estimation problem is *ill conditioned*. In this case the system identification process may produce wrong parameter estimates or may even fail since there are infinite combinations of parameters that lead to the same variation in the cost function. Troubles occur even if there is an almost linearly dependence among some parameters. In this case the difficulties increase when the dependence among the parameters approach to linear dependence.

There are several methods capable of detecting data collinearity [2, 9], but in this section only two of these will be presented.

3.6.1 *Correlation matrix*

The most simple method used to detect data collinearity requires a survey on the correlation matrix. In order to obtain the correlation matrix, the parameter error covariance matrix must be calculated. A suitable approximation for calculating the covariance matrix can be obtained [8] through the inverse of the Fisher information matrix, $\mathrm{Cov}(\theta) \approx \mathcal{F}^{-1}$ (see also 3.79).

Given an estimate of the covariance matrix, the element at position (p, q) of the correlation matrix, namely ρ_{pq}, is defined by

$$\rho_{pq} = \frac{d_{pq}}{\sqrt{d_{pp} d_{pq}}}, \tag{3.81}$$

where d_{pq} is the element at position (p, q) of the inverse of the Fisher information matrix.

The correlation matrix is obviously symmetric. Moreover the elements of the principal diagonal take the value 1, while the other elements are between -1 and 1.

If a coefficient d_{pq} is equal to $+1$ (or -1) then there is a perfect positive (negative) correlation between the parameters p and q, that means a perfect linear dependence and hence the presence of data collinearity.

Issues also arise when the coefficient d_{pq} approaches these values. Generally two parameters can be considered correlated when the absolute value of the coefficient d_{pq} is greater then $0,9$ (sometime $0,95$). In this case data collinearity occurs and the parameters p and q are considered not identifiable.

This method is very simple to use in order to detect collinearity, however small values for coefficients d_{pq} does not guarantee the absence of correlations among parameters.

Furthermore this method is not able to recognize when there is a correlation between more than two parameters. For this reason another method in the next section will be presented.

3.6.2 *Singular value decomposition*

A method used to detect a near linear dependence between more than two parameters uses the *singular value decomposition*

technique. Using this method, the Fisher information matrix can be decomposed as

$$\mathcal{F} = V\Sigma^2 V^T, \tag{3.82}$$

where Σ^2 is an $n \times n$ diagonal matrix whose elements σ_i^2 are the eigenvalues of the matrix $\mathcal{F}$, while V is an $n \times n$ orthonormal matrix whose columns are the eigenvectors of $\mathcal{F}$.

A method [4] that allows to obtain the decomposition in 3.82 will be presented in this section. This method is used because it is based on a stable numerical decomposition, and because it allows to calculate the inverse of the Fisher information matrix that is required if the methods analysed in the previous sections (for example Gauss-Newton) are used.

Let $\mathcal{H}$ the matrix be defined as follows

$$\mathcal{H} = \begin{bmatrix} R^{-1/2}G_1 \\ R^{-1/2}G_2 \\ \vdots \\ R^{-1/2}G_N \end{bmatrix}, \tag{3.83}$$

where R is the measurement error covariance matrix and $G_i = \partial y_i/\partial\theta$ are the output sensitivities. The singular value decomposition of the matrix $\mathcal{H} \in \mathbb{R}^{mN,n}$ leads to

$$\mathcal{H} = USV^T \tag{3.84}$$

where the matrix $U \in \mathbb{R}^{mN,mN}$ and $V \in \mathbb{R}^{n,n}$ are the left and the right orthonormal unit matrices of the decomposition. The matrix $S \in \mathbb{R}^{mN,n}$ can be written as follows

$$S = \begin{bmatrix} \Sigma \\ 0 \end{bmatrix}, \tag{3.85}$$

where Σ is a diagonal matrix whose elements σ_i, called *singular values* of $\mathcal{H}$, are non-negative and are sorted in descending order, i.e. $\sigma_1 \geqslant \cdots \geqslant \sigma_n \geqslant 0$.

The Fisher information matrix can be written using the matrix $\mathcal{H}$ as follows

$$\mathcal{F} = \mathcal{H}^T \mathcal{H} \tag{3.86}$$

Using the singular value decomposition and some properties of the matrix, the Fisher information matrix in equation 3.82 can be rewritten as

$$\mathcal{F} = V \Sigma^2 V^T.$$

The inverse of the Fisher information can be calculated using equation 3.82 in the following way

$$\mathcal{F}^{-1} = V \Sigma^{-2} V^T. \tag{3.87}$$

It can be seen that the Cramér-Rao inequality 3.80 can be rearranged as

$$\mathrm{Cov}(V^T \theta) \geqslant V^T \mathcal{F}^{-1} V, \tag{3.88}$$

that, with some calculations, leads to

$$\mathrm{Cov}(\Theta) \geqslant \Sigma^{-2}, \tag{3.89}$$

where $\Theta = V^T \theta$ is a new set of unknown parameters.

Equation 3.89 states that the diagonal elements of the matrix Σ^{-2} represent the lower bound for the new vector of parameters Θ. Therefore if an element of the matrix Σ^{-2} exceeds a certain value then data collinearity occurs and the corresponding parameter of Θ can be considered not identifiable.

Once the parameters considered not identifiable have been detected, they can be excluded from the optimization problem,

which can be performed only with the vector Θ_{id} of the identifiable parameters.

Finally the original vector of parameters θ can be calculated as follow

$$\theta = V\Theta.$$

4

IDENTIFICATION OF WIND TURBINES

In this chapter the methods used for identifying the aerodynamic characteristics of wind turbines will be described to obtain better estimates for such aerodynamic characteristics. As a result, these identified characteristics lead to a better correspondence between the experimental data and the data obtained from the theoretical model used to predict the performance of the wind turbines.

The identification of the aerodynamic characteristics of wind turbines is an important subject of research. This topic has been already discussed in the literature [1, 4] since the overall performance of a wind turbine strongly depends on the aerodynamic properties of the airfoils placed along the blades span and therefore it is fundamental to obtain reliable estimates for the aerodynamic characteristics.

Sometimes it happens that the real performance of the produced wind turbines do not correspond to the performance predicted by the used mathematical model during the design of the wind turbines themselves. The reasons that produce these discrepancies can be different and they are briefly reviewed below.

A first reason for these discrepancies is the mathematical model used to predict the performance of wind turbines. Indeed a mathematical model capable of reproducing the exact behaviour of a wind turbine does not exist and the theoretical

models used nowadays actually provide only an approximation on how the real wind turbines work.

The most common mathematical model used to predict the performance of a wind turbine is the blade element momentum (BEM) theory, described in details in chapter 2. It is based on some assumptions used to simplify the formulation of the mathematical model since it is very difficult to obtain a comprehensive model that is able to consider the totality of the phenomena involved in the operation of wind turbines. Therefore these assumptions that neglect some of the physics underlying the phenomena, prevent to take into consideration the exact behaviour of a wind turbine even though some corrections were provided to improve the fidelity of the model as it has been already described in chapter 2.

Another discrepancy between the experimental and the simulated data depends on the turbulence of the wind that is actually not modelled in the BEM theory and that is very hard to model in other simulation codes. Discrepancy between the experimental and the simulated data also depend on some aerodynamic phenomena that are not modelled by the BEM theory for example aeroelastic phenomena, dynamic stall and so on. Actually, there are some aerodynamic models that allow to consider such effects. However in this thesis work, the attention is focused mainly on the adjustment of the aerodynamic characteristics, that are believed, as stated in [11, 17], the major source of error in prediction of loads and performance.

Manufacturing errors can also lead to discrepancies in the data, since the aerodynamic characteristics, and consequently the loads and the overall performance too, are altered owing to the modified geometry of the airfoils placed on the blades. A

case in which manufacturing errors played an important role for the discrepancies between predicted and experimental data is described in details in section 4.4. In that section it is also described how the results given in output by the identification code are used to find the reasons that caused the discrepancies between predicted and experimental data.

Finally, another major reason for the discrepancies between experimental and predicted data is due to the fact that the mathematical models, for example the BEM theory used to reproduce the behaviour of the wind turbine in this thesis work, use two-dimensional characteristics for the airfoils placed along the blades span. These characteristics, that are true for two-dimensional steady flow around the airfoils, can be unreliable when rotating blades are considered. More the flow is far from being two-dimensional, more the experimental measurements differ from the predicted ones.

In fact some three-dimensional effects occur on the blades span. These effects influence the aerodynamic characteristics of the airfoils especially near the hub (that fortunately have less influence on the performance of wind turbines). As a result the two-dimensional aerodynamic characteristics, used to obtain the loads on the blades and therefore the performance of wind turbines, can be sometimes considered unreliable.

As pointed out in [1] several experiments have shown that a radial flow exist on the blades at the bottom of separated boundary layers. This phenomenon involves the alteration of the aerodynamic characteristics, namely the lift and the drag coefficients of the sections placed on the blades span. In particular it has been seen from experiments that the post stall lift increases on the inboard part of the blades (until $30-40\%$) in-

cluding the the drag, while the lift in the tip region decreases. This phenomenon is called *centrifugal pumping*.

Since the real aerodynamic characteristics experienced by the airfoils placed on the blades, as highlighted above, may differ from the supposed two-dimensional ones, a method that allows to find the aerodynamic characteristics really experienced by the wind turbine is needed.

In [1, 4] some methods are used to obtain reliable estimates for the aerodynamic properties. In those works the main difficulties related to the optimization process are also described. In particular those related to the great number of parameters, that is, however, required in order to guarantee a suitable variation of the different aerodynamic characteristics along the blades, and the difficulties due to the low level of identifiability of some parameters. Another difficulty that impedes the calculation of reliable estimates for the aerodynamic characteristics is represented by the so-called collinearity among parameters, which is described in details in chapter 3.

It has to be noted that the lift coefficient usually has a greater influence than the drag coefficient on the performance of wind turbines. Therefore the drag coefficient has generally a low level of identifiability and for this reason it is harder to identify. Tests conducted in this thesis work, and reported in the sections below, confirm the difficulty related to the identification of the drag coefficients. In fact, sometimes the identified drag curves don't change at all or they change so much to be considered unreliable. Furthermore, the performance of wind turbines is less influenced by the aerodynamic characteristics of the inboard sections rather than by the characteristics related to the sections placed on the tip of the blades.

For this reason the lift coefficient and even more the drag on the inboard sections have a low level of identifiability and therefore is difficult to obtain reliable estimates for such curves.

It also has to be noted that the identification of the characteristics related to the post stall angles of attack is usually hard to face since these angles are used only for particular working conditions and only for some sections. Indeed the post stall angles of attack are usually seen in the inboard sections, which have a low level of identifiability as already described above. Furthermore these angles of attack usually work only with low tip speed ratios, which means that these post stall angles can be seen only with few experimental measurements. For this reason reliable estimates for the aerodynamic characteristics related to such angles are very difficult to obtain.

The presence of a great number of parameters also leads to an unavoidable decrease of the possibilities to obtain reliable estimates. Hence a compromise between the possibility to change the aerodynamic characteristics and the need of reducing the number of parameters in order to improve the reliability of the obtained estimates has to be found.

In [4] the author tried to solve these problems using the singular value decomposition method that allows to obtain good estimates excluding the parameters that do not contribute to the identification of the aerodynamic characteristics through the Cramer-Rao lower bounds, described in chapter 3. Basically, if a lower bound exceeds a certain amount, then the related parameter is considered not identifiable and it is excluded from the identification problem. Thanks to this method the number of parameters is reduced and therefore the optimization problem is able to obtain more reliable estimates. This method also

contribute to reducing the correlations among parameters as described in chapter 3.

The purpose of this thesis work is to reduce the number of parameters a priori, by choosing suitable parametrizations for the aerodynamic characteristics that allows to avoid the growth of parameters and therefore the exclusion of them during the optimization problem.

The number of parameters to be identified is generally too high, since a great amount of them are needed in order to parametrize the different aerodynamic curves along the blades. This fact makes really hard the identification of the aerodynamic characteristics since it is usually accompanied by the low level of identifiability and by the great level of correlation among the parameters themselves. For this reason a reliable geometry parametrization is needed in order to reduce the number of parameters and to limit the correlation among parameters and the low level of identifiability.

The input and the output quantities related to the estimation problem will be briefly described hereinafter to improve the understanding of the parameters meaning and of the optimization problem target. The performance of wind turbines can be summarized using the fundamental characteristics curves C_P, C_Q and C_T, which are usually written as function of the tip speed ratio λ. A typical example of such curves is depicted in figure 5. These curves can also be used as function of the speed of the wind in order to identify the aerodynamic characteristics.

An example of identification of the aerodynamic characteristics of a wind turbine, where the experimental measurement provided is the power as function of the velocity of the wind, is performed in section 4.4.

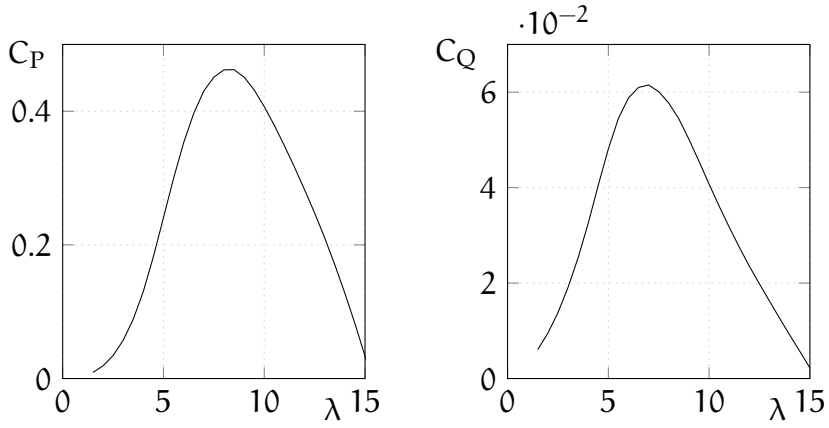

(a) Power coefficient

(b) Torque coefficient

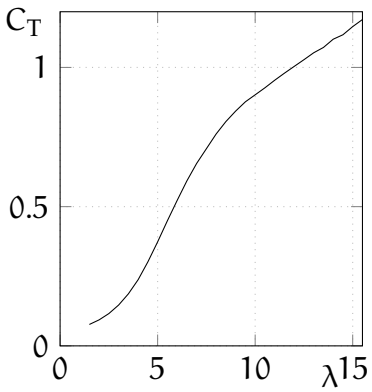

(c) Thrust coefficient

Figure 5: Typical characteristic curves

Once a wind turbine has been designed, and hence, for example, the radius and the distribution of twist and chord have been established, the fundamental characteristics curves, obtained for example by using the Bem theory, depends only on the aerodynamic characteristics, i.e. the lift and the drag coefficients of the airfoils placed along the blades span.

It is believed [11, 17] that the main source of errors for a wind turbine in the prediction of loads, and performance too, is due to the wrong aerodynamic characteristics used for the airfoils on the blades span.

For this reason and since the two-dimensional aerodynamic characteristics may not model, as highlighted before, in an adequate way the real behaviour of the airfoils, the aim of the application of the geometry parametrizations studied in this thesis work and in particular in this chapter is to simplify the research of reliable aerodynamic characteristics (C_l and C_d). This adjustment allows to obtain numerical performance that better correspond to the real performance by including for example the three dimensional effects and all the physical phenomena that are not described by the considered aerodynamic model. The fidelity of the mathematical model, and in the particular case of the BEM used in this thesis work, is therefore improved since better aerodynamic characteristics for the airfoils of the wind turbines can be considered.

A typical example of the lift and the drag coefficients curves of an airfoil is depicted in figure 6.

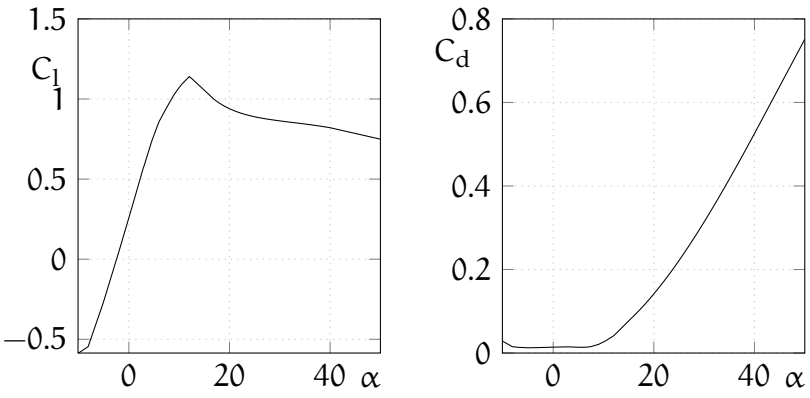

(a) Lift curve (b) Drag curve

Figure 6: Typical aerodynamic curves

The adjustment of the aerodynamic characteristics of the wind turbines is obtained through the methods of system identification which tries to fit the performance predicted by the used mathematical model with the real experimental performances,

by maximizing the probability of the realization of the experimental data as described in chapter 3.

The research of suitable aerodynamic characteristics is a very difficult task. Experimental measurements have usually little information content since only the power and sometimes the thrust coefficients are available and generally for only a closed range of angles of attack. The identification of the wind turbines Bora and EOL-H-60 performed in this thesis work has used only the experimental measurements related to the power.

For this reason the power and the thrust coefficients, that are, in addition, obtained integrating the aerodynamic characteristics as described in chapter 2, are very difficult to use in order to obtain reliable estimates for the parameters related to the identified aerodynamic characteristics.

The identification process can be numerically simplified taking also into account the loads on the blades span too, but practical applications of this method are very difficult to achieve since they require considerable changes on the wind turbines which must be provided with appropriate strain gauges which in turn must be suitably calibrated to obtain reliable estimates.

It is obvious that as the number of measurement data increases, the estimation of the parameters is improved, but in this thesis work only the evaluation of the power coefficient is considered because in most cases this coefficient is the only data that can be easily obtained, since it does not require any variation on the wind turbine. However in order to include also the thrust coefficient in the identification code, only little modifications on the software are needed.

It has to be noted that in [4] experimental measurements namely the power and the thrust coefficients are taken for dif-

ferent pitch angles. This fact improve the identification of the aerodynamic characteristics since a great informative content is taken into account and a broader range of angles of attack for the aerodynamic characteristics can be considered. It also has to be noted that not always all these experimental data can be provided since sometimes the geometry of some wind turbines cannot be easily modified. This is the case of stall controlled wind turbines where the pitch angle is fixed. The experimental measurements of the wind turbines studied in this thesis work are obtained for one pitch angle, both for the BORA that is a fixed pitch turbine and for the EOL-H-60 that is a variable pitch wind turbine.

4.1 GEOMETRY PARAMETRIZATION

A suitable method that allows changing the shape of the aerodynamic curves is needed since it is difficult to adjust these curves using its coordinates directly. Indeed the aerodynamic curves are made by several points and a great amount of parameters is required in the optimization problem if the points related to the aerodynamic curves are used as parameters without specific techniques.

Unfortunately, the presence of a great number of parameters usually lead to ill-conditioned problems in systems identification applications especially when the experimental measurements have little informative content as in the case of the wind turbines studied in this thesis work, where all the information is summarized in one or two curves. In such a case the methods of system identification can produce inaccurate aerodynamic characteristics, or may even fail. An example in which

the identification code has deliberately produced inaccurate results is described in section 4.2.4.

For this reason a suitable parametrization method has to be found in order to reduce the number of parameters of the optimization problem. In addition, this reduction of parameters must not prevent to obtain a parametrization able to reproduce different shapes for the aerodynamic curves, but at the same time it should contribute to avoiding the production of strange curves that have no physical meaning. Indeed it is very easy to obtain identified aerodynamic curves with strong oscillations, as it can be seen in the example declared above and described in section 4.2.4, if the parametrization method used is chosen without paying the right attention. This happens, as highlight above, because the output quantities are obtained by integrating the aerodynamic characteristics of the airfoils. Basically an oscillating curve has nearly the same output as a mean curve without oscillations because the increased parts of the given curve in a range compensates the reduced ones in its proximity in the integration process. The possibility to obtain such oscillations must be absolutely avoided. In the end the choice of such a parametrization must also try to reduce correlations among parameters in order to obtain more reliable estimates, even if these correlations can also be avoided through the use of the singular value decomposition method.

4.1.1 *Bezier Curves*

The geometry parametrization methods used to describe the shape of the different aerodynamic characteristics in this thesis

work are obtained through the use of the *Bezier Curves* in some different ways as described below.

In this thesis work the cubic, quadratic and the linear Bezier curves, which are based on the Bernstein polynomial, are used. They have respectively the following equations

$$B_3(t) = P_0(1-t)^3 + 3P_1t(1-t)^2 + 3P_2t^2(1-t) + P_3t^3,$$
$$B_2(t) = P_0(1-t)^2 + 2P_1t(1-t) + P_2t^2,$$
$$B_1(t) = P_0(1-t) + P_1t,$$

where $t \in [0, 1]$. The points P_i of the Bezier curves are called *control points*. Some of the coordinates of these points will represent the parameters of the optimization problem. An example of such these curves can be found in figure 7.

It has to be noted that the linear Bezier is nothing but a segment and its control points are the endpoints of the segment. The main properties of the Bezier curves are presented below.

- The derivative at the control points P_0 and P_{end} are respectively proportional to $P_1 - P_0$ and $P_{end} - P_{end-1}$.
- The curve lies inside the convex hull of its control points, as it can be seen in figure 8.

Different parametrization methods can be used to describe the aerodynamic curves. In this thesis work three specific techniques are used.

In the first method the aerodynamic curves are divided into two or more pieces, each of which is described by a Bezier curve. Basically this means to consider spline of Bezier curves. The choice of the number of pieces and of the degree of the Bezier curves is made by the user on the basis of experience

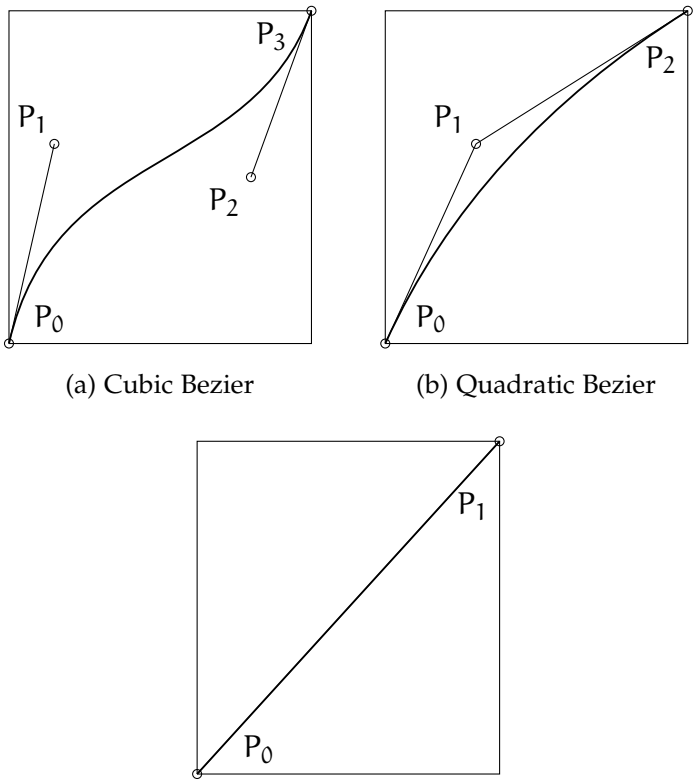

(a) Cubic Bezier (b) Quadratic Bezier

(c) Linear Bezier

Figure 7: Example of Bezier curves

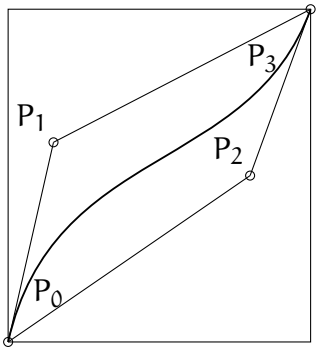

Figure 8: Convex hull of a Bezier curve

and after some attempts. A wrong choice can either bring to oscillating shapes and therefore can lead to the problems described hereinabove or give curves which are not able to reproduce in a suitable way the aerodynamic curves, for example because a little number of Beziers and therefore of parameters

is used. The choice depends firstly on the aerodynamic curve to be parametrized (lift or drag curves) and then on the amount of experimental data of the problem being considered. The choice must be done trying to describe in the best possible way the aerodynamic curves but, at the same time, avoiding considering an excessive number of parameters that will probably lead to wrong or inaccurate estimates.

In the second method a spline of Bezier is added to the initial numerical two-dimensional aerodynamic curves. A particular case of this method can be obtained using spline of linear Bezier and taking as parameters only the ordinates of their control points. This is the simplest way to parametrize the aerodynamic characteristics and it is also the parametrization method used in [4] and in [1]. Even if this method is quite simple and reliable, especially if linear Bezier are used, it is for example unable to change in a suitable way the stall angle of the lift curve.

The adjustment of the stall angle of attack in a easier way can be obtained by using the first method that, if suitably configured, is able to change the stall angle of attack. However this method allows to change the stall angle of attack only indirectly. For this reason another parametrization method, that allows to change in a direct way the stall angle of attack, is proposed.

It is obtained by using two quadratic Bezier. The last control point of the first Bezier is chosen so that it has a horizontal tangent. This point coincides with the first point of the second Bezier, that has a horizontal tangent too. Since the direction of the tangent at the last control point of the first Bezier is established by the direction of the segment made by the last and the second to last control points and the tangent at the first control point of the second Bezier is established by the direction of the

segment made by the first and the second control point, it is sufficient that these three points have the same ordinate to obtain the parametrization method required. The last control point of the first Bezier, that is the first point of the second Bezier, is exactly the stall angle of attack, and therefore its abscissa and its ordinate can be directly modified in the optimization problem.

Finally, the last part of the aerodynamic characteristics, that is the deep stall region and the most difficult part to identify as well, is parametrised using the semi-empirical method proposed by Viterna and Corrigan described in section 2.8. This chapter is divided into three parts.

In the first part some virtual experiments will be performed to verify the goodness of the identified characteristics produced by the identification code. An example in which the optimization problem returns wrong estimates is presented too.

In the second part some tests will be conducted in order to identify the aerodynamic characteristics of a real wind turbine. The wind turbine whose characteristic are identified in this part is the $2,5kW$ Bora designed by the the ADAG group of DIAS of the UNIVERSITY OF NAPLES FEDERICO II.

Finally in the third part the aerodynamic characteristics related to the wind turbine EOL-H-60 will be identified.

The following identification tests will be performed in the next sections; the virtual one and the real ones.

At first only one lift curve, used on the entire the blade span will be identified, assuming the drag coefficient equal to the numerical two-dimensional one.

Then one lift and one drag curve, considering again the same curve for all the blade span, will be identified.

Finally an identification is performed by dividing the blade into two sections for each of which the lift and the drag coefficients are identified.

4.2 VIRTUAL IDENTIFICATION

In this section some virtual tests are carried out to verify the goodness of the estimates provided by the software created during the doctoral studies.

At first, the presence of only one airfoil is supposed. Actually this assumption is unrealistic, since wind turbines are usually designed with several airfoils along the blade span. Furthermore even if the same airfoil is used on the blade, different aerodynamic characteristics should be used because the aerodynamic characteristics also depend on the Reynolds number, which usually changes along the blade span. However this is the simplest case and it is useful to start considering this configuration. It can be also used for example when the general case does not provide reliable estimates or when a first estimate for the aerodynamic characteristics is needed.

4.2.1 *Identification of the lift coefficient*

In this test the presence of only one airfoil is supposed, as stated above. Furthermore the drag coefficient is assumed to be known without errors. This means that the drag coefficient will not be included in the identification problem. So the identification of the only lift coefficient has to be performed.

In order to obtain *virtual* experimental measurements, the numerical aerodynamic characteristics, in this case the lift coeffi-

cient, is altered and hence the performance of the wind turbine with this new lift coefficient are used as the experimental measurements. Then the identification problem is performed with these (virtual) experimental data.

In the figures below, the numerical curves, those are the design curves, will be indicated by dotted lines. The experimental measurements, that are obviously available only for virtual tests and whose knowledge is the target of the research of this thesis work, will be indicated by dashed lines. Finally the identified values are indicated by solid lines. The initial value passed to the identification code is represented by the numerical aerodynamic characteristics while the target of the identification code is to provide as output the aerodynamic characteristics used to obtain the *virtual* experimental performance.

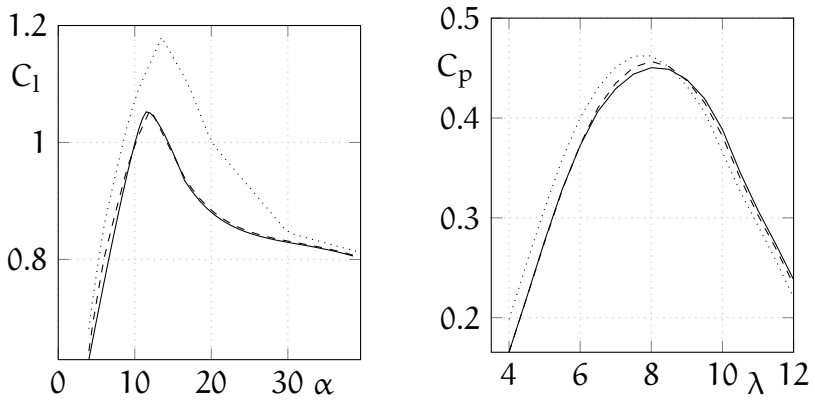

(a) Lift coefficient (b) Power coefficient

Figure 9: Identification of the lift coefficient of a wind turbine. Solid lines: identified curves; dashed lines: *virtual* experimental curves; dotted lines: initial curves.

In figure 9 the result of an identification problem can be found. As it can be seen, the alteration of the aerodynamic characteristics leads obviously to a variation of the performance of the wind turbine. The numerical curve was given in input to

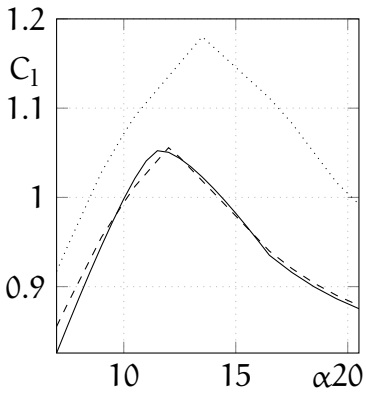

Figure 10: particular of the identified lift curve

the software. This software, using the methods of the maximum likelihood, tries to change the lift coefficient in order to obtain a curve whose performance is closer to the *virtual* experimental curve as output. The test has shown a good congruity between the experimental performance and the identified performance. In particular the code has been able to provide as output a lift curve quite similar to the *virtual* experimental lift curve used to obtain the *virtual* experimental performance.

4.2.2 *Identification of the lift and the drag coefficients*

In this section the lift curve is identified together with the drag curve of an airfoil belonging to a wind turbine blade. Always only one airfoil for all the blade span will be assumed. The number of parameters is obviously increased because in this case the parametrization of another curve is needed. The results can be seen in figure 11. It shows a good congruity between the virtual measurements and the identified ones. Furthermore, it can be seen that there is a good congruity between the numerical and the identified aerodynamic characteristics. In this case too the identification code has provided good estimates for the

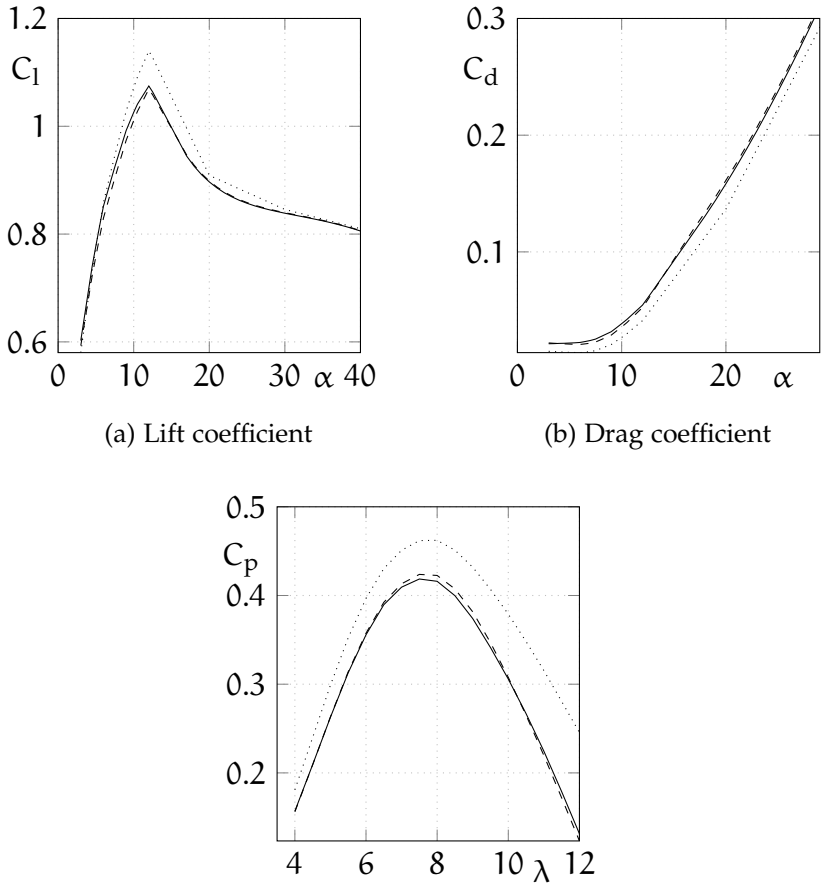

(a) Lift coefficient

(b) Drag coefficient

(c) Power coefficient

Figure 11: Identification of the lift coefficient and the drag coefficient of a wind turbine. Solid lines: identified curves; dashed lines: *virtual* experimental curves; dotted lines: initial curves.

aerodynamic curves that can be, at least in these case, therefore considered reliable.

4.2.3 *Identification of the aerodynamic characteristics of two airfoils*

The identification of the aerodynamic properties of two airfoils is far more difficult. This difficulty is due to the increase of the number of parameters used to parametrise four curves (two lift

curves and the two drag curves) although the number of experimental measurements does not change. A direct method of identification, that makes use of all the parameters as they are, sometimes fails because of the strong correlations among parameters and the low level of identifiability of themselves that unavoidably happens when the number of the parameters increases. Other methods, for example the single value decomposition method, give better results but are sometimes unable to identify some parameters. This failure is not due to the method itself (single value decomposition for example) but to the actual difficulty related to the identification of the aerodynamic characteristics. It has to be noted that the existence of only one solution cannot be guaranteed. Indeed, given a wind turbine, there can be two (or more) set of aerodynamic properties that give the same performance, as it can be seen in the simpler example of section 4.2.4. The loads on the wind turbine obviously change but they are not accessible without more invasive measurements. The results provided by the identification code are depicted in figure 12. It can be seen that the aerodynamic characteristics related to the airfoils placed in the root sections are not so well identified. This is due to the low level of identifiability of the airfoils placed in the inboard part of the blades, as stated in the previous sections. Regarding the tip curves it can be seen that the identified curves give good estimates only before the stall angle of attack.

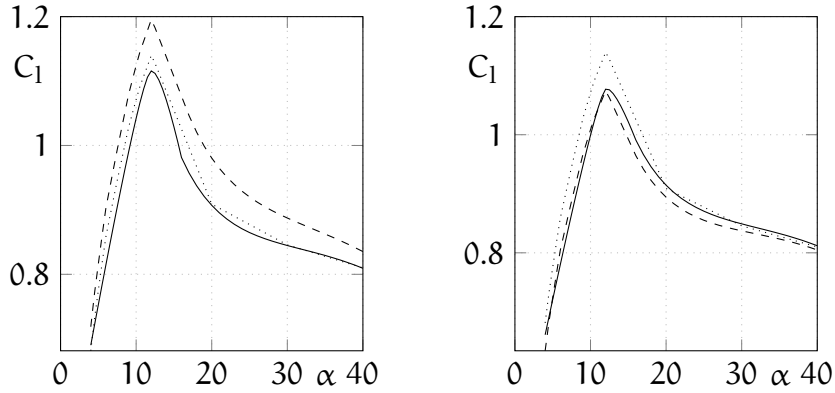

(a) Root lift coefficient

(b) Tip lift coefficient

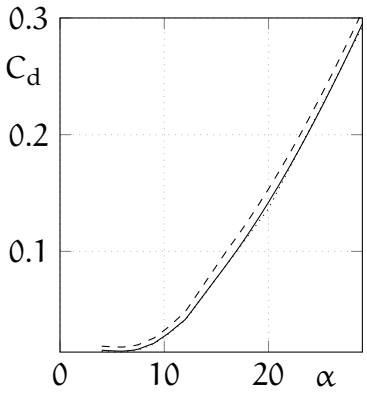

(c) Root drag coefficient

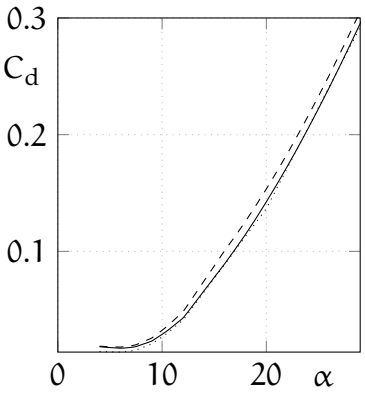

(d) Tip drag coefficient

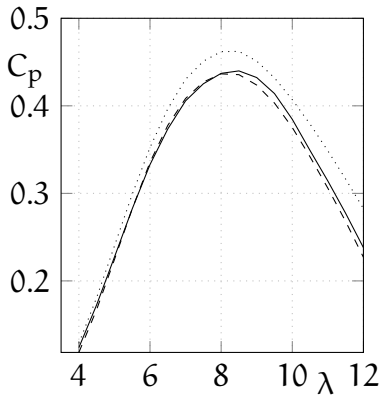

(e) Power coefficient

Figure 12: Identification of the lift coefficient and the drag coefficient of a wind turbine. Solid lines: identified curves; dashed lines: *virtual* experimental curves; dotted lines: initial curves.

4.2.4 *A simple case in which the identification of the aerodynamic characteristics is lost*

This section describes an example that emphasizes how important is the choice of a suitable parametrization method. In fact, as for the case showed below, if a wrong parametrization method is used, inaccurate results might be produced. Generally a great number of parameters can help to obtain a wide variety of curves and therefore a better approximation of the curve itseft, but at the same time it makes really hard the identification of the aerodynamic characteristics because the algorithm of the optimization problem makes a lot of efforts in order to identify all the parameters. The configuration used in this section is similar to that related to the example already seen at the section 4.2.1. Indeed in both cases the curve to be identified is only one lift curve that is assumed the same for the entire blade span. The differences between the two configurations are due to the method used to parametrize the lift curve. In section 4.2.1 the third method described in section 4.1.1 is used while in this section the first one, described in section 4.1.1, is used. In particular in this section two four-point Bezier are used to parametrize the lift curve, therefore 11 parameters are generated instead of the five parameters created section 4.2.1. The choice of two four-point Bezier is not very suitable because it makes more difficult the identification of the lift curve. The parameters created by the identification code do not have a strong ability to excite the system in a suitable way, in particular the parameters related to the second Bezier, used to parametrize the post stall region.

The results of the test can be found in figure 13.

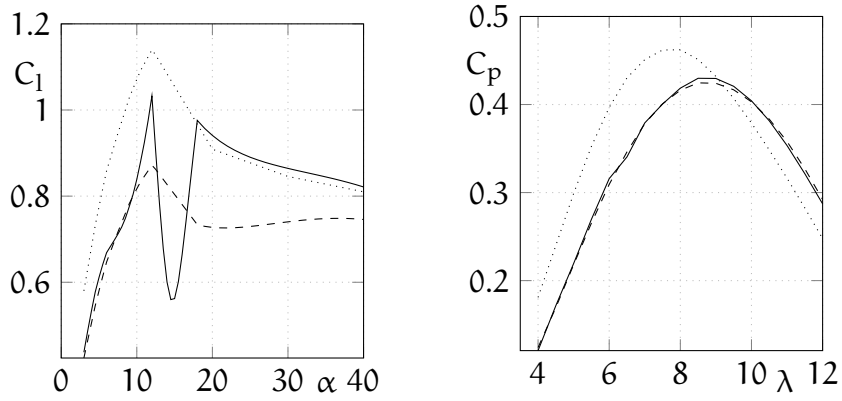

(a) Lift coefficient

(b) Power coefficient

Figure 13: Failure of an identification of the lift coefficient of a wind turbine. Solid lines: identified curves; dashed lines: *virtual* experimental curves; dotted lines: initial curves.

It can be seen that the optimization problem is quite able to identify the overall performance in a very reliable way. However the identified aerodynamic characteristics do not correspond to the virtual aerodynamic characteristics used to create the virtual experimental measurements. The example performed in figure 13 shows that the identification code was unable to find a reliable estimate for the lift curve, but it also shows a fundamental thing. It shows that, depending on the method used to parametrise the curve, the optimization problem related to the identification code generally have not only a global minimum, but it can have local minima too, reached in this case. Indeed the example depicted in figure 13 clearly shows the presence of two aerodynamic characteristics that have, with a good degree of approximation, the same performance. Obviously the identified curve cannot be considered reliable but, at the same time, important considerations can be made analysing the curves. Nevertheless the the identified curve do not correspond to the virtual one, the first part of the curve,

until 10 degrees, is quite close to the virtual experimental curve and it can be accepted. However the post stall region is extremely unreliable. Even in this case useful considerations can be made. Since the performance of a wind turbine is obtained through the integration of the lift curve, it can be seen that the identified curve oscillates around the real (in this case virtual) curve that can be considered a sort of mean curve of the identified one. Indeed the identified characteristics that exceed the virtual ones are compensated by the characteristics staying below the virtual curve.

4.3 IDENTIFICATION FROM EXPERIMENTAL DATA

In this section some identification trials are performed in order to find the aerodynamic characteristics of a real wind turbine: the horizontal axis wind turbine of 2.5 kW called Bora, developed by the ADAG group of DIAS of UNIVERSITY OF NAPLES FEDERICO II. The same trials that were performed with a virtual wind turbine in the previous sections will be carried out in the following. Obviously the experimental lift and drag cannot be reported, as for the previous sections, because they are unknown and they are exactly the curves proposed to be found in this thesis work. In addition, the performance data, belonging from experimental measurements are affected by an unavoidable measurement noise. For this reason they do not follow a smooth curve.

4.3.1 *Identification of the lift coefficient*

In this section, only one lift curve will be identified. This fact is unrealistic, as reported in the previous sections, but it can be useful to start from this case since this represents the simplest trial. This case can be used for example when the identification of the next sections gives unreliable estimates.

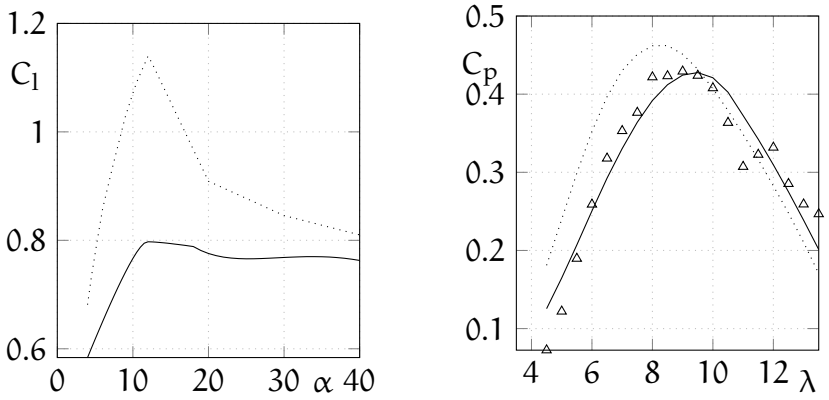

(a) Lift coefficient (b) Power coefficient

Figure 14: Identification of the lift coefficient of the Bora wind turbine. Solid lines: identified curves; points: experimental data; dotted lines: initial curves.

As it can be seen in figure 14, there is an acceptable congruity between the experimental performance and the identified performance. However this congruity is obtained through a dramatic reduction of the lift coefficient. Probably this is due to the fact that in this case the drag curve is not identified and it might be that a part of the experimental measurement depends on an increase of the drag itself. The identified curve represents the curve that, according to the bem theory, allows to obtain the performance that better approximate the experimental measured performance. Recall that the lift curve is obtained at first

parametrizing the curve itself: in this way a vector of parameters is created. These parameters are then used to identify the lift curve of the wind turbine using the maximum likelihood method, eventually combined with the singular value decomposition method if the parameters show a little degree of identifiability or a great level of correlation.

4.3.2 *Identification of the lift and the drag coefficients*

The next step is the identification of both the lift and the drag coefficient, assuming the presence of only one airfoil along all the blades span of the wind turbine.

The identified curves can be found in figure 15. In this trial, a reduction of the lift coefficient can also be observed. The results also show a reduction of the drag coefficient, contrary to expectations. Sometimes, because of the parameters correlations, the identification code instead of increase the drag of the airfoils, decreases the lift curve, obtaining a similar result. However the identified performance show a good congruity with experimental measurements, thus this result cannot be rejected a priori.

4.3.3 *Identification of the aerodynamic characteristics of two airfoils*

In this section the lift and the drag coefficients pertaining to the Bora wind turbine will be identified. Differently from the last section, this one has the presence of two airfoils. On the one hand this assumption improves the degree of the aerodynamic characteristics approximation, since a more realistic configuration can be considered. On the other hand this assumption causes the increase of the number of parameters and leads

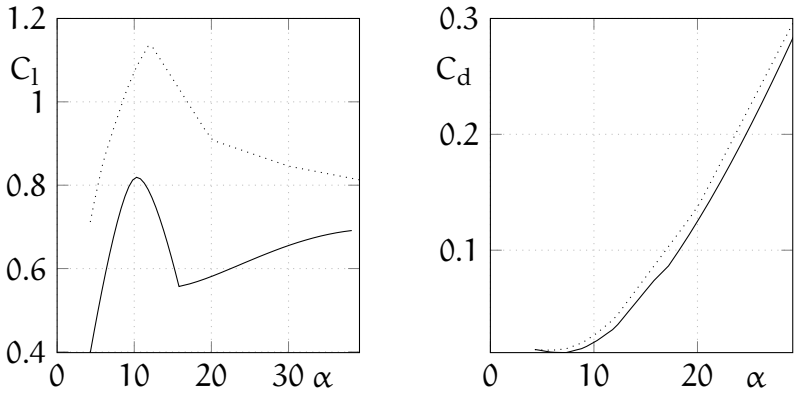

(a) Lift coefficient

(b) Drag coefficient

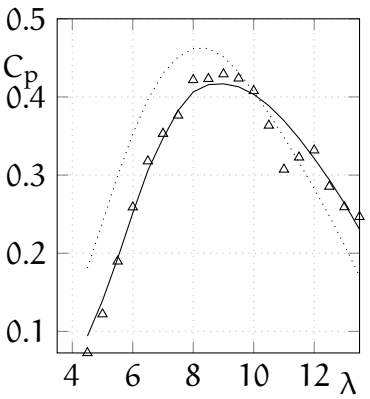

(c) Power coefficient

Figure 15: Identification of the lift coefficient and the drag coefficient of the Bora wind turbine. Solid lines: identified curves; points: experimental data; dotted lines: initial curves.

therefore to an unavoidable reduction of the degree of parameters identification and in addition, it leads to an increase of the correlations among them.

As it can be seen in figure 16 there is a little reduction of the lift coefficient at the root sections and there is a greater reduction of the lift coefficient at the tip sections. One can also observe that the drag coefficients are affected by really few changes. This fact is due to the singular value decomposition method.

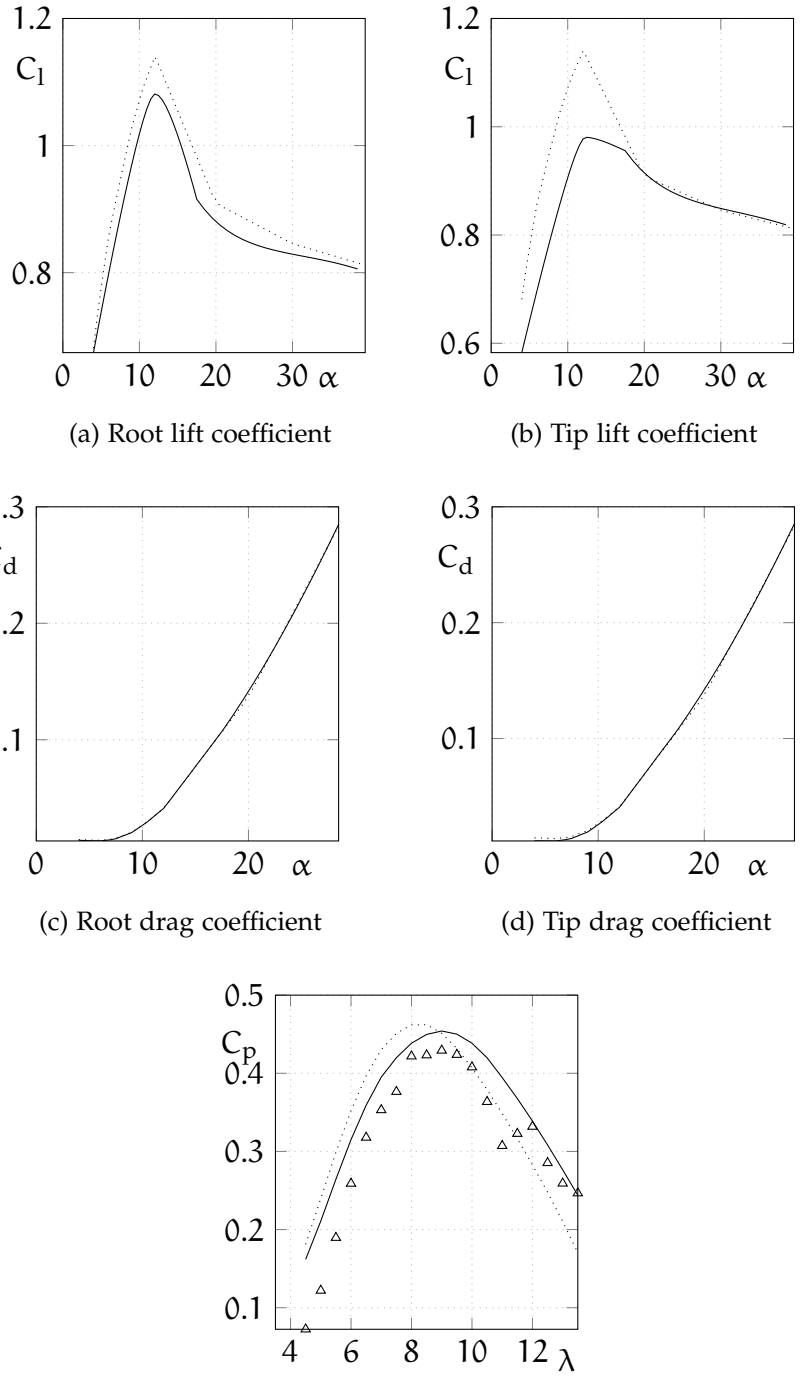

(a) Root lift coefficient

(b) Tip lift coefficient

(c) Root drag coefficient

(d) Tip drag coefficient

(e) Power coefficient

Figure 16: Identification of the lift coefficient and the drag coefficient of the Bora wind turbine. Solid lines: identified curves; points: experimental data; dotted lines: initial curves.

Furthermore the identified performance are not so close to the experimental measurement. Therefore this identification cannot be considered fully reliable.

Another attempt was performed to identify the aerodynamic characteristics of the lift and the drag coefficients related to two airfoils. In this case the software was forced to give a better congruity between experimental measurements and identified performance taking into account a greater number of parameters. However, these parameters have a lower level of identifiability.

The result is shown in figure 17.

In this case, a greater congruity be observed between identified performance and experimental measurement. However the identified aerodynamic properties show a greater change than the previous identification case. It can be seen in figure 17, that there is an increase of the lift curve at the root sections as expected. Indeed, this fact confirm the presence of the centrifugal pumping, already discussed in the previous chapters. It states that the inner sections are affected by a growth of the lift curve. The presence of the centrifugal pumping can also be seen in the previous test since the reduction of the lift curve related to the root section was less pronounced that the reduction of the one related to the tip sections. This phenomenon is not modelled by the bem theory, but it can be included by properly modifying the table of the lift coefficients. The lift coefficient related to the tip sections also shows a greater reduction in this test, as expected.

Regarding the drag coefficient a great increase of the characteristics related to the tip sections can be observed. Whereas, only a slight increase in the characteristics related to the the root sections is observed. The reasons for the slight increase of

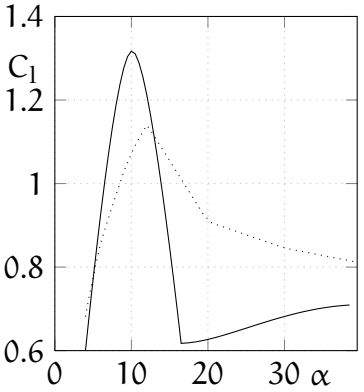

(a) Root lift coefficient

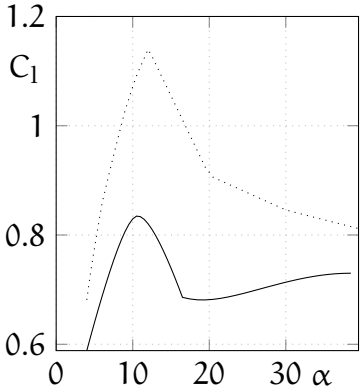

(b) Tip lift coefficient

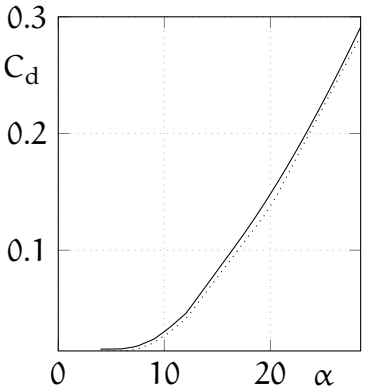

(c) Root drag coefficient

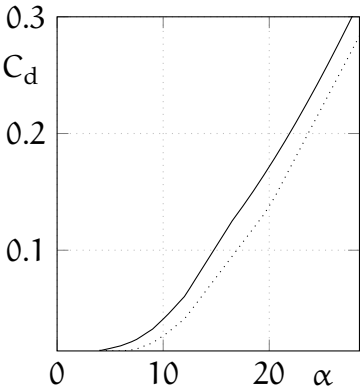

(d) Tip drag coefficient

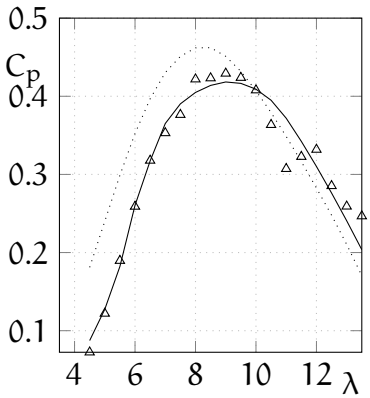

(e) Power coefficient

Figure 17: Identification of the lift coefficient and the drag coefficient of the Bora wind turbine. Solid lines: identified curves; points: experimental data; dotted lines: initial curves.

coefficients related to the root section can de due to the low level of parameters identifiability related to that curve.

4.4 IDENTIFICATION OF THE WIND TURBINE EOL-H-60

In this section the identification of the wind turbine of 60 kW EOL-H-60, developed by the ADAG group of DIAS of UNIVERSITY OF NAPLES FEDERICO II in partnership with COMECART S.p.a. of Cuneo, is performed. The EOL-H-60 showed considerable discrepancies (about 30%) between the predicted performance and the experimental ones, as it can be seen in figure 18.

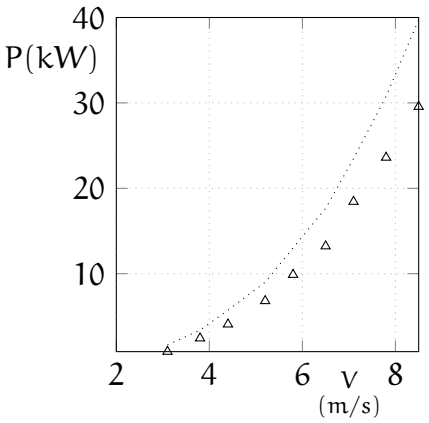

Figure 18: Discrepancies between experimental and predicted data of the wind turbine Eol-H-60. Triangles: experimental data; dotted line: predicted curve.

Therefore, the identification code developed in this thesis work, was performed to find the reasons underlying such discrepancies and attempt to fix them. The identification of the EOL-H-60 was somewhat difficult, because the experimental data are derived from measurements taken on the field, according to the international standard IEC 61400-12-1 [7]. However, the obtained data are unable to properly excite the parameters to be

identified. In this case, the experimental measurements taken for the identification of the aerodynamic characteristics of the EOL-H-60 are not the coefficients of power C_p over λ, but the power P over the velocity of the wind V_∞.

The wind turbine operates in such a way that the rpm of turbine itself are adjusted to obtain a specific value of lambda, because for that lambda, the wind turbine is able to extract the maximum quantity of energy from the wind. This fact means that only the aerodynamics characteristics related to few angles of attack are experienced by the airfoils and therefore only these aerodynamic characteristics can be identified, even if a wider range of angles of attack will be plotted below.

4.4.1 *Identification of the lift coefficient*

In this section the identification of one lift curve related to the wind tubine EOL-H-60 is performed. The results of the identification are shown in figure 19. There is a fair congruity between the identified performance and the experimental one. It can be seen that the identified lift curve (actually, the part of the lift curve best identified is the part of curve related to the α between 0 and 10 degrees since the other values have not been excited by the system in a suitable way) is shifted downward and/or to the right, with respect to the numeric lift curve. The reasons of these motions are described below.

4.4.2 *Identification of the lift and the drag coefficients*

In this section, the identification of one lift and one drag curve related to the wind turbine EOL-H-60 is performed. The results

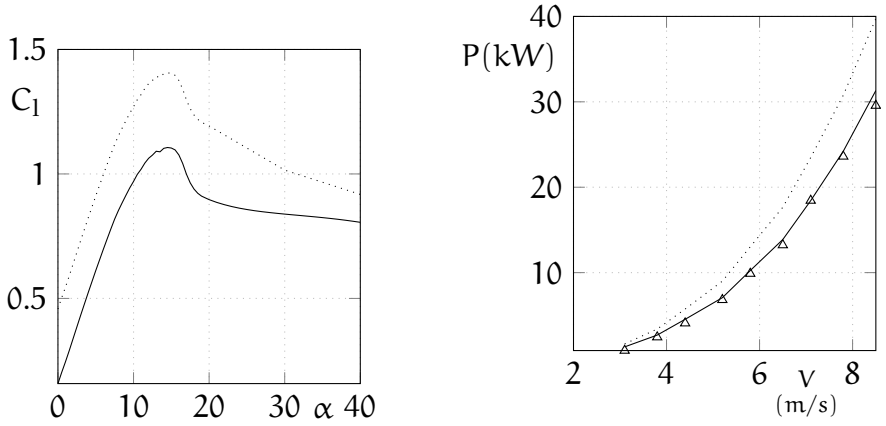

(a) Lift coefficient

(b) Power coefficient

Figure 19: Identification of the lift coefficient of the EOL-H-60 wind turbine. Solid lines: identified curves; triangles: experimental data; dotted lines: initial curves.

of the identification are shown in figure 20.

Figure 20 shows that there is a fair congruity between identified and experimental data. As in the case of the previous section, it is observed that the lift curve is shifted downward or (and) to the right with respect to the numeric lift curve. Since in this case the lift and the drag coefficients are both identified, it is certainly possible to observe an increase of the drag coefficients, that is very pronounced, but possible as well. It can be due to phenomena that are not been described by the model used to calculate the performance, for example the vibrations of the blades that are not modelled by the blade element momentum theory.

4.4.3 *Conclusions*

In this section the results of the previous tests are discussed. Firstly, as stated hereinabove, it has to be noted that the predic-

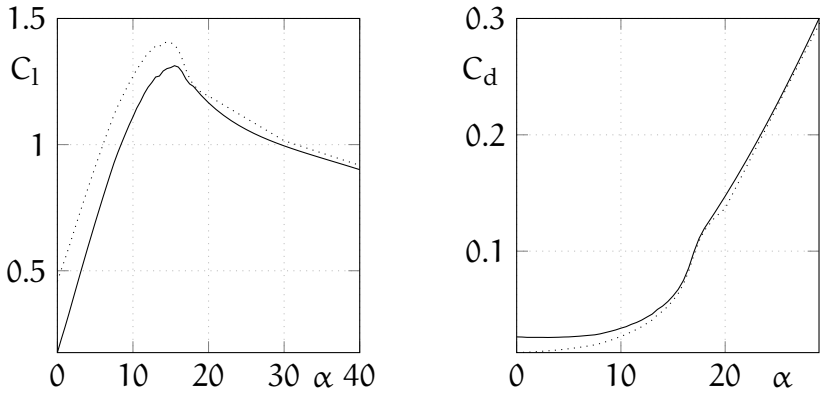

(a) Lift coefficient

(b) Drag coefficient

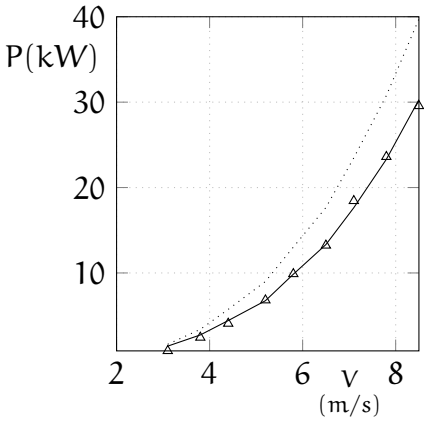

(c) Power coefficient

Figure 20: Identification of the lift and the drag coefficients of the EOL-H-60 wind turbine. Solid lines: identified curves; triangles: experimental data; dotted lines: initial curves.

tion code WTPERF, that uses the blade element theory to calculate the performance, has shown that the angles of attack experienced by the airfoils are mostly included in the range between 0 and 10 degrees. Therefore, only the aerodynamic characteristics related to these angles of attack can be identified and can be considered reliable. The lift curve related to the identified range of alpha is depicted in figure 21. As stated above, the identified curve is shifted downward and/or to the right. This translation has an aerodynamic meaning and it can depend on several fac-

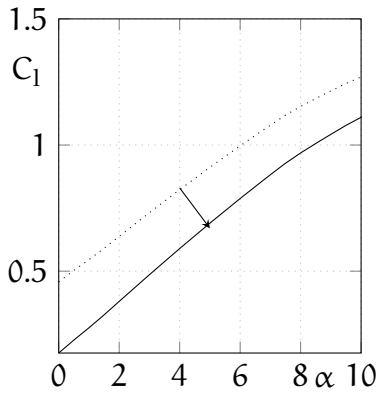

Figure 21: Particular of the identified lift curve. Solid line: identified curve; dotted line: numerical curve.

tors. For example, the motion of the lift curve shown by the results of the identification code can be due to a mistake in the real shape of the airfoils placed on the blades. This can happen when manufacturing errors occur, in particular when the airfoil bottom is too pronounced because it causes the alteration of the curvature of the airfoil and therefore the change of the α_0 lift. In addition, the motion of the lift curve, depicted in figure 21, can also be due to a wrong pitch angle of the blades placed on the wind turbine, since this corresponds to a translation to the right or to the left of the aerodynamic properties.

An analysis on the wind turbine EOL-H60 has showed both these problems. New blades, with the bottom airfoil less pronounced, were produced to fix the problem of the increased α_0 lift, related to the translation to the right of the lift curve. Furthermore, the pitch angle of the blades was adjusted to fix the motion of the lift curve, since it can also be considered another source of the alteration of the α_0 lift. After making these adjustments, new experimental measurements have been taken. These measurements can be seen in figure 22.

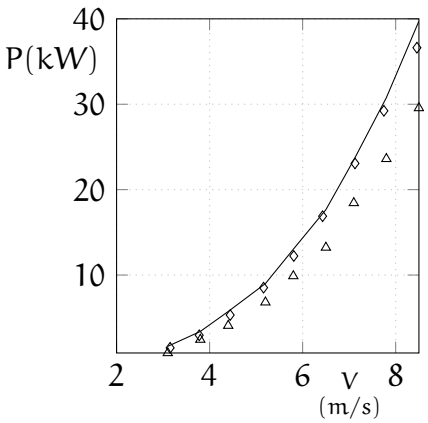

Figure 22: Discrepancies between experimental and predicted data of the wind turbine Eol-H60 after the adjustments of the blades. Triangles: experimental data before corrections; diamonds: experimental data after corrections; dotted line: predicted numerical curve.

As it can be seen from figure 22, the new experimental measurements obtained after the adjustments, better correspond to the numerical performance. This means that the results given by the identification code are able to provide useful suggestions to correct potential manufacturing errors and therefore to improve the performance of wind turbines, even if the identification of the aerodynamic characteristics of wind turbines sometimes gives faulty results (depending on the parametrization method chosen and the number of curves identified) due to the nature of the inverse problems that are usually *ill-conditioned*, in particular the identification of the aerodynamics characteristics of wind turbines that shows both the problem of the low level of identifiability of some parameters and a strong correlation among them.

BIBLIOGRAPHY

[1] Bak, C. et al. "Airfoil Characteristic for Wind Turbines". In: *Risø National Laboratory, Roskilde, Denmark* (1999).

[2] Belsley, D. A., Kuh, E., and Welsh, R. E. *Regression Diagnostics: Identifying Influential Data and Sources of Collinearity*. Wiley, New York, 1980.

[3] Burton, T., Sharpe, D., Jenkins, N., and Bossanyi, E. *Wind Energy Handbook*. John Wiley & Sons, Ltd Eds, 2001.

[4] Cacciola, S. "Wind Turbine System Identification and Stability Analysis". PhD thesis. Politecnico di Milano, 2012.

[5] Drela, M. "XFOIL: An Analyse and Design System for Low Reynolds Number Airfoils". In: *Low Reynolds Number Aerodynamics, Springer Verlag Lecture Notes in Engineering, Vol. 54* (1989).

[6] Hoener, S.F. *Fluid Dynamic Drag: Practical Information on Aerodynamic Drag and Hydrodynamic Resistance*. Hoerner Fluid Dynamics, 1965.

[7] "IEC 61400-12-1 Wind turbines- Part 12-1: Power performance measurements of electricity producing wind turbines." In: *International electrotechnical commission* (2005).

[8] Jategaonkar, R. V. *Flight Vehicle System Identification: a Time Domain Methodology*. AIAA, 2006.

[9] Klein, V. and Morelli, E. A. *Aircraft System Identification Theory and Practice*. AIAA, 2006.

[10] Ljung, L. *System Identification: Theory for the User*. Prentice Hall, 1987.

[11] Moriarty, P. J. "AeroDyn Theory Manual". In: *National Renewable Energy Laboratory* (2004).

[12] Ostowari, C. and Naik, D. "Post Stall Studies of Untwisted Varying Aspect Ratio Blades with an NACA 4415 Airfoil Section - Part I". In: *Wind Engineering* (1984).

[13] Ostowari, C. and Naik, D. "Post Stall Studies of Untwisted Varying Aspect Ratio Blades with an NACA 4415 Airfoil Section - Part II". In: *Wind Engineering* (1985).

[14] Ostowari, C. and Naik, D. "Post-Stall Wind Tunnel Data for NACA 44XX Series Airfoil Sections". In: *SERI/STR 217-2559* (1985).

[15] Platt, A. D. and Jr. Buhl, M.L. "Wt perf user guide for version 3.05.00". In: *Technical report, National Renewable Energy Laboratory* (2012).

[16] Tangler, J. L. "A Horizontal Axis Wind Turbine Performance Prediction Code for Personal Computers(User's Guide)". In: *Solar Energy Research Institute* (1987).

[17] Tangler, J. L. "The Nebulous Art of Using Wind Tunnel Aerofoil Data for Predicting Rotor Performance". In: *Wind Energy* (2002).

[18] The MathWorks, Inc. *MATLAB and Statistics Toolbox*. Natick, Massachusetts, United States, 2015.

[19] Tognaccini, R. *Lezioni di aerodinamica dell'ala rotante, eliche, rotori ed aeromotori.* Department of Aerospace Engineering, University of Naples Federico II, 2011.

[20] Viterna, L. A. and Corrigan, R. D. “Fixed pitch rotor performance of large horizontal axis wind turbines.” In: *NTRS* (1982).

[21] Viterna, L. A. and Janetzke, D. C. “Theoretical and Experimental Power from Large Horizontal-Axis Wind Turbine”. In: *NASA* (1982).

[22] Zadeh, L. A. “From Circuit Theory to System Theory”. In: *Proceeding of the IRE* (1962).